Experimental Testing of PEM Electrolyzer Degradation

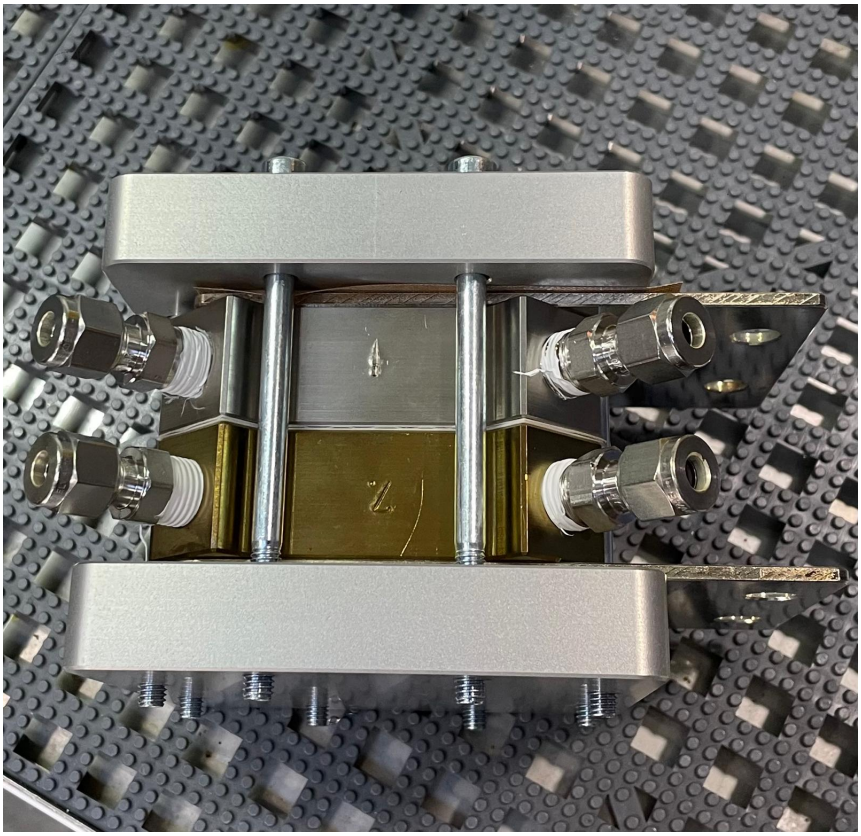

Project Report
Group HYTEC3-911

Aalborg University
Energy

Energy
Aalborg University
Pontoppidanstræde 101/111
9220 Aalborg Øst
https://www.energy.aau.dk/

Title:
Experimental Testing of PEM Electrolyzer Degradation

Theme:
Water Electrolysis

Project Period:
Autumn Semester 2025

Project Group:
HYTEC3-911

Participant(s):
Javier Bermúdez Blanco

Supervisor(s):
Vincenzo Liso
Co-supervisor:
Hamilton Delaney Miller

Page Numbers: 57

Date of Completion:
December 16, 2025

Abstract:

Green hydrogen plays an important role in the technological development of sustainable energy. PEM electrolyzers are one of the most promising technologies to produce green hydrogen. However, more research is needed to develop this technology. One of the biggest concerns about the PEM electrolyzers is its degradation over time. Therefore, this project investigates degradation mechanisms under laboratory conditions. Experimental cells were manually assembled and subjected to long term testing using the Greenlight Innovation test station. Unfortunately, an internal electrical short circuit was present throughout all the experiment, which negatively impacted the data obtained. It was identified and fixed at the end of the experiment
The study characterized reversible and irreversible degradation mechanisms. The electrolyzer reached a performance peak at 264 hours of operation, after which an efficiency decrease due to degradation was observed. The irreversible degradation was linked to chemical ionomer degradation, PTL passivation, catalyst dissolution, and carbon corrosion. The performance increase at higher temperatures and the independency of water flow rate and pressure variations was proven. Reversible losses, primarily caused by bubble accumulation, were consistently observed and recovered through shutdown. A stress test on carbon-based Porous Transport Layers (PTL) confirmed their incompatibility with the Oxygen Evolution Reaction (OER).

Preface

This report is made by Javier Bermúdez Blanco, student of the 3rd semester of the master's degree in Fuel Cells and Hydrogen Technology at Aalborg University. The program subject is *Project in Advanced Energy Systems*, and the elected project is *Experimental Testing of PEM Electrolyzer Degradation*.

The supervisor in charge of this project is Vincenzo Liso, and the co-supervisor is Hamilton Delaney Miller, who guided the laboratory experiment and provided useful literature review and material list summary. Also mention the help of Fan Zhou in the laboratory. Thank you for all the work done to make this project possible.

Reading Guide

Throughout the project, citation of sources occurs in sequential numerical order. The sources are collected in a bibliography at the end of the project. Figures follow a chapter based numbering system, i.e. the first figure in chapter 3 would be figure 3.1, the next one would be figure 3.2, and so on. Figures have a caption that describes them.

A table with a list of symbols to define the nomenclature is presented in page V.

Aalborg University, December 16, 2025

Javier Bermúdez Blanco
jbermu24@student.aau.dk

Nomenclature

List of symbols

SI units are used.

Symbol	Definition	Unit
ΔH_f^o	Reaction formation enthalpy	$\frac{\text{kJ}}{\text{mol}}$
ΔG^o	Gibbs free energy	$\frac{\text{kJ}}{\text{mol}}$
V_{th}^o	Thermoneutral potential	V
z	Number of electrons transferred	e^-
F	Faraday constant	$\frac{\text{C}}{\text{mol}}$
V^o	Reversible potential	V
m	Mass	kg
I	Electrical current	A
t	time	s
M	Molar mass	$\frac{\text{g}}{\text{mol}}$
ϵ	efficiency	%
$\dot{n}$	Molar flow	$\frac{\text{mol}}{\text{s}}$
λ	Number of water molecules per sulfonic acid site	-
ω	Weight percentage	%
EW	Equivalent weight	-
J	Flow	$\frac{\text{mol}}{\text{s}}$
n_{drag}	Drag coefficient	$\frac{\text{mol}}{\text{m}^2\cdot\text{s}}$
n_{cell}	Number of cells	-
j	Current density	$\frac{\text{A}}{\text{cm}^2}$
D^{eff}	Diffusion coefficient	$\frac{\text{m}^2}{\text{s}}$
$\text{D}_{\Delta P}$	Transport coefficient	$\frac{\text{mol}}{\text{Pa}^2\cdot\text{m}\cdot\text{s}}$
D_{drag}	Drag coefficient	$\frac{\text{mol}}{\text{Pa}\cdot\text{C}}$
t_{mem}	Membrane thickness	m
υ	Water velocity	$\frac{\text{m}}{\text{s}}$
C	Concentration	$\frac{\text{mol}}{\text{L}}$
ΔP	Pressure difference	Pa
P_x	Partial pressure	Pa
V	Voltage	V
η	Overvoltage	V
W_t	Electrical work	kJ
e^-	Free electron	-

Chemical compounds

Symbol	Definition	Unit
HER	Hydrogen evolution reaction	-
PEM	Proton exchange membrane	-
PEMWE	Proton exchange membrane water electrolyzer	-
M	Metal	-
BPP	Bipolar plate	-
PTL	Proton transpor layer	-
CL	Catalyst layer	-
MEM	Membrane	-
GDL	Gas diffusion layer	-
OER	Oxygen evolution reaction	-
PTFE	Polytetrafluoroethylene	-
EIS	Electrochemical impedance spectroscopy	-

Subscripts

Subscript	Meaning
l	Liquid phase
g	Gaseous phase
x	Substance "x"
op	Produced
$theo$	Theoretical
F	Faradaic
th	Thermoneutral
eod	Electro-osmotic drag
$diff$	Diffusion
$conv$	Convection
act	Activation
ohm	Ohmic
$conc$	Concentration
max	Maximum

Chemical compounds

Chemical representation	Meaning
H_2O	Water
H_2	Hydrogen
H^+	Hydrogen proton
O_2	Oxygen
OH^-	Hydroxide
H_3O^+	Hydronium ion
Pt	Platinum
Fe	Iron
SO_3H	Sulfonic acid
CO_2	Carbon Dioxide
C	Carbon
Ti	Titanium
Cu	Copper
Au	Golf
IrO_2	Iridium dioxide
IrO_x	Iridium oxides
RuO_2	Ruthenium Dioxide
NO_x	Nitrogen oxides
NH_3	Ammonia
NH_4^+	Ammoniun
S	Electrochemical active site

Contents

1 Introduction **1**

2 Problem Statement **2**
2.1 Project limitations . . . 2

3 State of Art **3**
3.1 PEM Electrolyzer . . . 3
3.2 Degradation . . . 4

4 Theory **6**
4.1 Electrolyzer principles . . . 6
4.2 Faraday's Law . . . 8
4.3 Electrolyzer Overview . . . 8
4.3.1 Bipolar Plates . . . 9
4.3.2 Porous Transport Layer . . . 9
4.3.3 Anode Catalyst Layer . . . 9
4.3.4 Proton Exchange Membrane . . . 10
4.3.5 Cathode Catalyst Layer . . . 12
4.3.6 Gas Diffusion Layer . . . 13
4.3.7 Operating Conditions . . . 13
4.4 Electrolyzer Characterization . . . 14
4.4.1 I-V curve . . . 14
4.4.2 Efficiency . . . 15
4.4.3 Lifetime . . . 16
4.5 Degradation Theory . . . 17
4.5.1 Chemical Ionomer Degradation . . . 17
4.5.2 Ionomer Inhibition . . . 18
4.5.3 Passivation . . . 18
4.5.4 Mechanical Membrane Degradation . . . 19
4.5.5 Platinum Catalyst Degradation . . . 19
4.5.6 Iridium Catalyst Degradation . . . 19
4.5.7 Carbon corrosion . . . 20
4.5.8 Reversible Degradation . . . 20

5 Experiment Description **21**
5.1 Electrolyzer components . . . 21
5.1.1 Membrane . . . 21
5.1.2 PTL . . . 22
5.1.3 GDL . . . 22
5.1.4 Flow Plates . . . 22
5.1.5 Gaskets . . . 23
5.1.6 Current Collectors . . . 23

5.2 Break in/Conditioning . . . 24
5.3 Data measured . . . 24
5.3.1 EIS . . . 25

6 Experiment Procedure **27**
6.1 Cell assembly . . . 27
6.2 Cell pretreatment . . . 28
6.3 Leaking test . . . 28
6.4 Initial test . . . 28
6.5 Break in/Conditioning . . . 29
6.6 Electrolyzer operation . . . 29
6.7 Data analysis . . . 29

7 Results and Discussion **30**
7.1 Initial test . . . 30
7.2 First experiment . . . 32
7.2.1 Test 1 . . . 32
7.2.2 Test 2 . . . 32
7.2.3 Test 3 . . . 35
7.2.4 Test 4 . . . 37
7.2.5 Test 5 . . . 38
7.2.6 IV comparison . . . 39
7.3 Second experiment . . . 40
7.4 Degradation experiment . . . 43
7.5 Degradation overview . . . 44
7.6 Electrolyzer malfunctioning . . . 45
7.7 Electrolyzer with no electrical short circuit . . . 46
7.7.1 IV curve . . . 46
7.7.2 EIS . . . 47
7.8 Model . . . 48
7.8.1 Exchange current density . . . 48
7.8.2 Resistances . . . 49
7.8.3 Faradaic efficiency . . . 50

8 Conclusion **51**

9 Future Work **52**
9.1 Experimental set-up . . . 52
9.2 Longer and continuous experiment . . . 52
9.3 Operation conditions . . . 52
9.4 Model development . . . 52

Bibliography **53**

Appendix **i**

1 Introduction

Hydrogen as an energy carrier is an emerging technology that promises to reduce the environmental impact of fuels. Due to the green energy status of hydrogen and the increasing price of fossil fuels, hydrogen has become one of the most promising technologies to achieve the energy transition goals.
There exist different technologies to produce hydrogen. It is mainly obtained from fossil fuels, such methane steam reforming, from electricity by electrolysis, and from waste or industrial byproducts. [1] [2]

One of the most promising ways of producing hydrogen is by electrolysis, where water and electricity obtained from renewable sources are used as feedstock. This process is a zero-emission process which is carried out in a device called electrolyzer. Nowadays, around 4% of all hydrogen produced comes from water electrolysis.[1]

The biggest challenges which this method of producing hydrogen has to face are the economic viability and the process energy efficiency. In consequence, research is needed to develop this technology and enable its widespread adoption. Electrolyzers are usually expensive due to the high-cost materials which are needed to build the cell, such as iridium, platinum or other rare materials. The bipolar plates made of titanium represent around 50% of the total stack cost. Different alternatives are being studied to reduce the cost of the electrolyzer.[2]

Another factor that affects the electrolyzer efficiency over time and increases its cost is the degradation, similarly to fuel cells, it reduces the lifetime of the device and decreases its performance. This is an important matter of study in the field. Currently, the lifetime of a PEM electrolyzer is around 40,000-60,000 hours, with a target of 120.000 hours by 2050. [2] [3]

Regarding the degradation in PEM electrolyzers, the catalyst layers and the membranes are the components most affected by degradation, so it is crucial to understand how they behave in different scenarios and which one is the most efficient one. Therefore, an experimental study of the proton exchange membrane and cell degradation at different operation conditions is of great importance to assess performance losses.

Problem Statement 2

Based on chapter 1, a problem statement can be made:

How can PEM electrolyzer degradation be experimentally measured and to what extent it affects electrolyzer performance?

To find the solution to this question, the following specific objectives are stated:

- Theoretical description of PEM electrolyzer and degradation.
- Setup and procedure of the experiment.
- Data analysis and conclusions.

2.1 Project limitations

The experiment is limited by different factors, such as:

- There is a limited time to carry out the experiment.
- Temperature limitations.
- Single cell operation.
- Steady state operation.

State of Art 3

3.1 PEM Electrolyzer

Electrolysis is a well-known technology with more than 100 years of usage in the industrial field, it was invented in 1789 by Dutchmen Jan Rudolph Deiman and Adriaan Paets van Troostwijk, and NorsK Hydro started to produce large-scale electrolyzers in the 1920s.[4][1]

Proton exchange membrane electrolyzer technology development is directly connected to the discovery of perfluorinated ion-exchange Nafion membranes. The first PEM electrolyzers were created in the 1960s by General Electric. [5]
PEM electrolyzers were first used for oxygen production in anaerobic environments, but with the advancement of this technology and the necessity of energy storage, it began to be used for hydrogen production. Today, there exist industrial large-scale electrolyzers, 1-10 MW, and even larger ones are being developed (10-100 MW).

One of the main drawbacks of this technology is the price, electricity prices and precious metals which are used as catalysts have a huge impact on the price. The precious materials used are mostly iridium, ruthenium, and platinum based materials. Some possible variations are being studied to reduce the price of an electrolyzer. [6]
New materials with great projection are being studied as catalyst support materials, they are mostly nanomaterials made from electrospinning which have a high specific surface area and electrical conductivity, and enhance catalysts performance. [7]
Non-precious materials are also being studied as the current catalyst replacement, these are Fe, Ni, Co... based materials which will reduce the PEM electrolyzer cost and facilitate its scalability. [8]

Literature states that conventional electrolyzers operate at 30 bar and 50-90°C, and it recommends not exceeding 50 bar of pressure for safety reasons. Temperature could be increased more but the electrolyzers and membranes used nowadays are designed for liquid water operation, not vapor.
One goal for the future is to operate the electrolyzer at very high pressures (200-300 bar), it has been already operated at pressures up to 350 bar. Nevertheless, the gas crossover makes these configuration not impractical through time. [6]

3.2 Degradation

In terms of PEM degradation, different studies have been carried out to try to predict and model the behaviour of the PEM in an electrolyzer.

In 1998 Stucki et al.[9] concluded that the membrane is the weakest part of electrolyzer for long operation time. It was also found that the membrane degradation depends on the position within an individual cell or on the cell position in a stack.

Later on, Luan et al.[10] confirmed that chemical instability is one of the factors that affect the most to the electrolyzer assembly degradation. Different models have been developed to try to predict the membrane thinning over time, e.g. Chandesris et al.[11] presented a model of PEM degradation considering the electrochemical degradation and studying the behaviour at different current densities and temperatures. Most of the degradation models are based on the fluoride released rate.
More research is needed to be able to implement degradation models to PEM electrolyzer systems, as it was remarked in the study conducted by Ashkan Makhsoos et al.[12] in 2025. They explain different model techniques for obtaining a realistic degradation model of the cell different parts at different scales. These models, validated with empirical data, would help to develop more accurate and robust models which maximize the PEMEW efficiency, reliability and lifetime.

In recent history, various PEM degradation factors have been studied at different conditions and stress levels. Eva Wallnöfer-Ogris et al.[2] identified different degradation mechanisms and the impact of them on the cell components at different operating conditions.

Marco Bonanno et al.[13] studied the performance and degradation of PEM electrolyzer at elevated temperatures (90°C) in 2024. They concluded that high temperatures increase the drop in PEM conductivity and chemical decomposition rates, but it reduces the amount of energy demanded, the catalyst loading, and the utilization of noble materials.

Eveline Kunhert et al.[14] studied the effect of hydrogen crossover in membrane degradation doing accelerated stress tests at 60 and 80°C. They found more H_2 content in the O_2 stream, a higher fluoride emission rate and a considerably higher degree of membrane thinning at 80°C. A more stable behaviour was observed at 60°C, where the degradation rate is significantly lower, and even a decrease in H_2 crossover was observed at low current densities. In conclusion, H_2 crossover plays an important role in membrane degradation, and higher temperatures stimulate the crossover rate.

A very recent study by Bernhardt et al.[15] from 2025 summarizes the most important degradation mechanisms. They are arranged in terms of impact on the membrane. It shows that the mechanisms which affect the most to membrane degradation are PTL passivation, anode catalyst dissolution, membrane thinning by radical attack, catalyst particle loss/layer detachment,membrane mechanical degradation, BPP corrosion, cathode catalyst dissolution and membrane metal poisoning.

Foniok et al.[16] also made an extended study about the degradation mechanisms in 2025.

They studied the chemical, mechanical and electrochemical degradation, as well as other cell components degradation. They also describe the three best methods to model degradation: physically based, data-driven and hybrid models. They concluded that it is necessary to develop advanced perfluorinated membranes that resist free radicals and catalysts with ultra-low platinum content, to reduce costs and improve durability. It is also essential to implement real-time dynamic models.
Figure 3.1 shows the schematic overview of the degradation mechanisms and the affected components.

Figure 3.1. Degradation processes and mechanisms overview [16]

Eva Wallnöfer-Ogris et al. [17] conducted a great review of all the most important degradation mechanisms, their causes, and how to mitigate the effects. These mechanisms will be described in the next chapter.

Theory 4

4.1 Electrolyzer principles

Water electrolysis is the process of splitting water into hydrogen and oxygen by applying an electrical current, as the global reaction in equation (4.1) shows: [4]

$$H_2O_{(l)} + \Delta H_f{}^\circ \rightarrow H_{2(g)} + \frac{1}{2}O_{2(g)} \qquad \Delta H_f{}^\circ = 285.8\frac{kJ}{mol} \tag{4.1}$$

This reaction is an endothermic reaction, which means it is necessary to supply energy for the reaction to happen. $\Delta H_f{}^\circ$ is the reaction formation enthalpy at standard conditions (25°C and 1 atm), and the Gibbs free energy of the reaction (ΔG°) is $237.1\frac{kJ}{mol}$.
The energy is given to the system in the form of electricity. The thermo-neutral potential (V_{th}^o) needed can be calculated using equation (4.2), which takes into account the reaction formation enthalpy, the number of electrons transferred (z = 2) and the Faraday constant (F=96,485 $\frac{C}{mol}$).[4][18]

$$V_{th}^o = \frac{\Delta H_f{}^\circ}{z \cdot F} = 1.48V \tag{4.2}$$

This parameter represents the voltage which needs to be supplied to reach thermo-neutral conditions. So the reaction would happen without external heating or cooling, at isothermal conditions. It does not consume or release heat. If the cell operates at higher potential than 1.48V, it would operate at exothermic conditions.

The reversible potential (V^o) or minimum theoretical thermodynamic voltage is calculated using the Gibbs free energy, as shown in equation (4.3):

$$V^o = \frac{\Delta G^\circ}{z \cdot F} = 1.23V \tag{4.3}$$

This parameter gives the minimum electrical potential needed for the water splitting at standard conditions. More energy should be applied to overcome the kinetic losses, and make the reaction happen, trying to reach the thermo-neutral potential. But, in real life, there are actually more losses, such as contact and solution resistances, ohmic losses, or mass-transport limitations.
Therefore, in order to have high energy efficiency, it is of great importance to reduce these losses as much as possible by using a suitable and stable catalyst and choosing optimum operation conditions. [4][18]

For the water splitting reaction to happen, two main-half reactions occur. Firstly, in the anode, the water molecules are split into oxygen and hydrogen protons, freeing electrons.This

reaction (equation (4.4)) is called oxygen evolution reaction (OER): [4][18]

$$H_2O \longrightarrow 2\,H^+ + \frac{1}{2}\,O_2 + 2\,e^- \tag{4.4}$$

This reaction can be described by the Krasilshchikov mechanism:[4]

$$S + H_2O \longrightarrow S{-}OH_{abs} + H^+ + e^- \tag{4.5}$$

$$S{-}OH_{abs} \longleftrightarrow S{-}O^- + H^+ \tag{4.6}$$

$$S{-}O^- \longleftrightarrow S{-}O + e^- \tag{4.7}$$

$$2\,S{-}O \longleftrightarrow 2\,S + O_{2(g)} \tag{4.8}$$

Where S is the electrochemically activate site of the electrode.

Then, oxygen is removed from the electrolyzer and the hydrogen protons cross to the cathode side through the membrane. The free electrons move from the anode to the cathode through an external circuit.[4]

In the cathode side, the hydrogen evolution reaction (HER) takes place between the cathodic catalyst layer and the membrane to form hydrogen molecules from hydrogen protons and electrons. Equation (4.9) shows this reaction:[4][18]

$$2\,H^+ + 2\,e^- \longrightarrow H_2 \tag{4.9}$$

HER is one of the simplest reactions, since it is a one reaction step for the electron transfer, no chemical bonds are formed or broken so the geometry of the species is constant, and no intermediates, products or starting materials are absorbed on the electrode.
Nevertheless, the HER reaction mechanism is not completely understood because it varies a lot depending on the materials and operation conditions. The next mechanism is overall accepted to describe the HER:[4]

1. Transport of water molecules to the phase boundary and adsoprtion.
2. Change transfer to the catalyst. The Volmer-Tafel mechanism is the one selected to describe this process.

   2.1.Volmer step: formation of adsorbed hydrogen atoms, reaction in catalyst surface.

   $$H_3O^+ + S + e^- \longleftrightarrow S{-}H + H_2O \tag{4.10}$$

   2.2.Tafel step: recombination of adsorbed H atoms

   $$M{-}H + M{-}H \longleftrightarrow 2\,M + H_2 \tag{4.11}$$

3. Desorption of H_2 molecules from the catalyst surface.
4. Removal of H_2 gas, by diffusion, convection and/or gas bubble formation.

There are other mechanism that describe the step number 2, such as the Volmer–Heyrovsky or the Reversed Heyrovsky–Tafel. But the most widely used one is the one presented above.

4.2 Faraday's Law

Faraday's Law describes the relation between the amount of gas produced and the charge consumed by the electrolyzer in electrochemical reactions. So, it is possible to calculate the amount of hydrogen produced by using the Faraday's Law: [4]

$$m = \frac{I \cdot t \cdot M}{z \cdot F} \tag{4.12}$$

Where m is the mass of gas produced, I is the electrical current, t is the time, M is the molar mass of the gas, z is the number of electrons transferred per mol of gas produced, and F is the Faraday constant (F = 96485 C).
The value obtained applying Faraday's Law is the ideal theoretical value. The faradaic efficiency (ϵ_F) of the electrolyzer can be calculated using the following equation:

$$\epsilon_F = \frac{\dot{n}_{H_2,op}}{\dot{n}_{H_2,theo}} \tag{4.13}$$

Being $\dot{n}_{H2,op}$ the hydrogen produced and $\dot{n}_{H2,theo}$ the theoretical hydrogen produced, in mol/s.

4.3 Electrolyzer Overview

This process of water electrolysis is carried out on a device called electrolyzer. An electrolyzer is a cell that can be divided into anode, electrolyte, and cathode.The anode is formed by a bipolar plate (BPP), a proton transport layer (PTL) and a catalyst layer (CL).
The cathode is also composed of a bipolar plate and a catalyst layer, but instead of having a PTL it has a gas diffusion layer (GDL). Figure 4.1 shows a representation of the different parts of an electrolyzer and the main reactions that occur in the anode and cathode, as well as the flow directions.

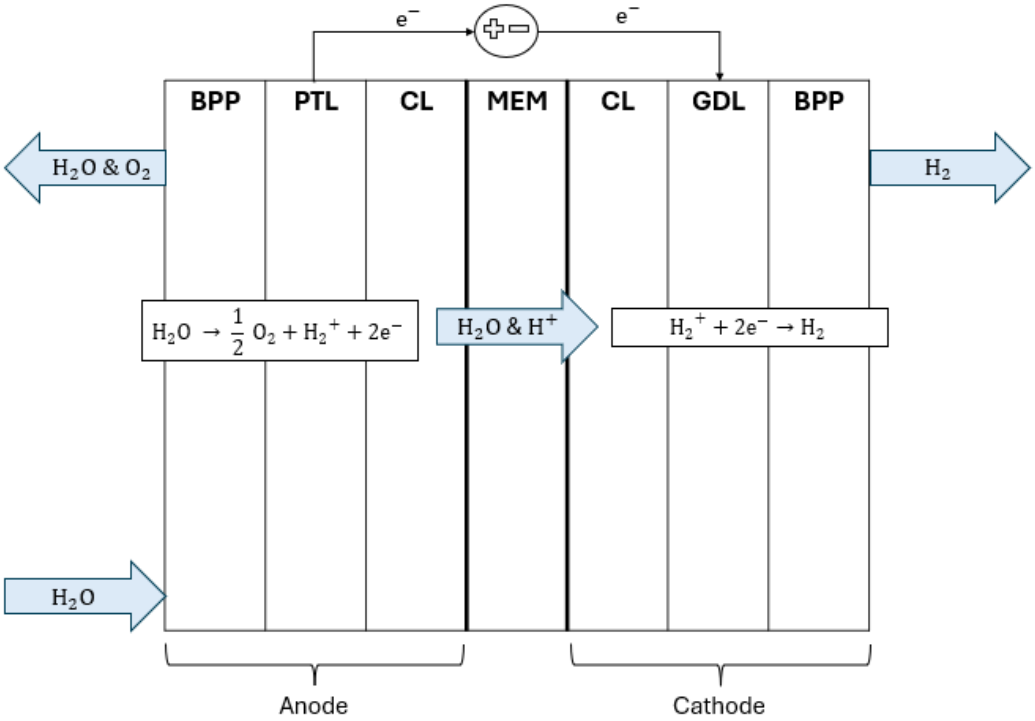

Figure 4.1. Electrolyzer representation

4.3.1 Bipolar Plates

Bipolar plates are structures placed at both ends of the PEM, in the anode and in the cathode. They are multifunctional components, their main goal is to properly distribute the water flow in the cell and to do a rapid removal of the gaseous phases. It also works as a mechanical support for the cell, and it separates single electrolyzers in a stack, conducting heat and electricity from one electrolyzer to another.[18]

Bipolar plates represent around 80% of the cell weight, 50% of its volume, and 50% of the cell price. They must be made of a highly corrosion-resistant material, they have historically been made of graphite, but it tends to be oxidized to CO_2 at high current voltages. So, corrosion-resistant metals with high thermal and electrical conductivity are being studied and used, such as stainless steel, titanium and their alloys.[18]

4.3.2 Porous Transport Layer

The porous transport layer is located in the anode between the bipolar plate and the catalyst layer. This component is in charge of providing mass transport pathways for the gas-liquid phase, as well as conducting electricity and heat, from the bipolar plate to the catalyst layer and vice versa.[18]

The PTL must be made of a material which presents a high-corrosion resistance, great electrical and thermal resistance, low contact resistance with other components, convenient pore and porosity, and thin thickness for gas removal. Titanium-based materials are the material selected in the porous transport layer since they fulfill all the above-mentioned conditions.

The porosity and thickness control is usually useful in the optimization of the electrolyzer, large pores spaces decrease the two-phase transport and high porosity increases the porous transport layer resistance. It is also important to have a low contact resistance between PTL and CL, to stimulate the flow transport. Pore diameter between 10 and 13 μm and open pore size around 0.2mm multilayer titanium PTL were found to be optimum.[18]

Microporous layers with titanium particles are used to decrease the loading of catalyst, since they increase the active sites of the catalyst by penetrating into the pores in the PTL. Consequently, the performance of the cell increases.
Coating materials on the surface of the PTL can also be used to increase the lifetime of the cell. Platinum and gold can be used for this purpose.[18]

4.3.3 Anode Catalyst Layer

The anode catalyst layer is an iridium, ruthenium or both iridium and ruthenium based oxide layer which works as a catalyst for the OER. It is located between the PTL and the PEM, it must facilitate the transport of water, gaseous oxygen, protons and electrons, and it must be resistant to highly acidic and oxidizing environments due to the presence of electrons and the operation conditions. This is why precious metals are the most suitable option. [6]

The most used catalysts are IrO_2, RuO_2 and IrO_2-RuO_2. IrO_2 has a higher corrosion

resistance, but is less active than RuO_2, which performs better at low potentials.They can also be mixed to obtain a more stable catalyst with mixed properties. However, the IrO_x catalyst is the most common one, it is presented in two forms, amorphous and crystalline, being the amorphous form more active and less durable. The usual loading of anode catalyst is around 1.24 mg/cm^2.[18][6]

Nevertheless, it is necessary to find other high-active robust materials to progress in the PEM electrolyzer implementation on the MG-scale commercialization, since iridium and ruthenium are highly demanded, and expensive materials.[18]

4.3.4 Proton Exchange Membrane

The proton exchange membrane is a solid polymer that acts as an electrode in electrolyzers, it is located between the two catalyst layers. Its purpose is to serve as a bridge for the hydrogen protons to cross from the anode to the cathode, maximizing the proton conductivity. It also compartmentalizes the oxygen gas in the anode and hydrogen in the cathode, preventing gas crossover. [6] [18]

Perfluoridic acid (PFSA) membranes, such as Nafion, Aciplex or Flemion, are the most used today thanks to the characteristics they present. They have a compact design with chemical-mechanical stability, a good water uptake and moderate swelling, they can operate at high-pressure and they present a very good proton conductivity at high operation temperature (90^{o}C). [18]

Nafion is the most widely used because of its high proton conductivity. The phase separation between the hydrophobic polymer backbones and the hydrophilic side chains terminated by sulfonic and functional acid groups (-SO_3H) is the reason why protons can move efficiently through the membrane. They usually have a thickness of 100 μm, but new membranes present a reduction to 25 μm thanks to the incorporation of inorganic antiparticles, increasing efficiency and conductivity. Figure 4.2 shows the structure of a Nafion membrane: [18] [19]

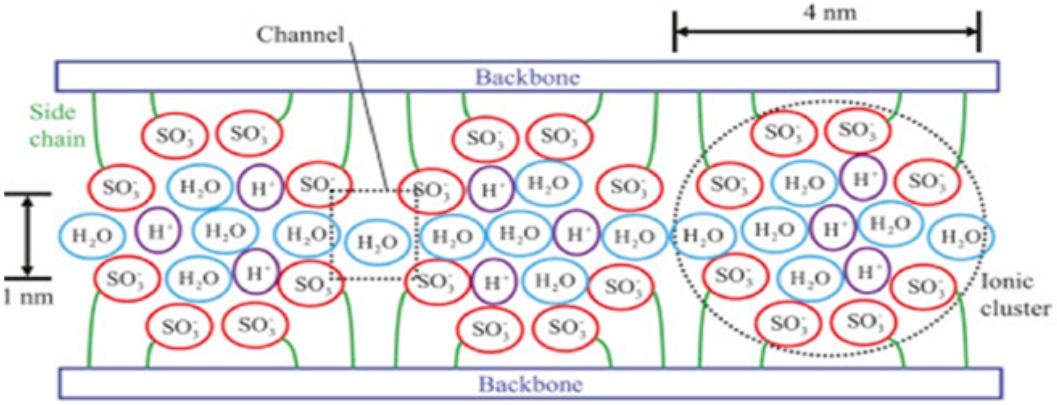

Figure 4.2. Nafion membrane structure [19]

The membrane must be hydrated to stimulate the proton conductivity, water flows through the membrane due to the electro-osmotic drag and the diffusion. The parameter called water

uptake(λ) represents the number of water molecules per sulfonic acid site: [4][20]

$$\lambda = \frac{\omega \cdot EW}{M_{H_2O}} \tag{4.14}$$

ω is the weight percentage of water in the membrane, EW is the equivalent weight of Nafion, and M_{H_2O} is the water molar weight. The proton conductivity is directly proportional to the water uptake when $2< \lambda <22$, at $\lambda = 22$ the membrane fully hydration is reached.

There are two mechanisms which describe the proton conduction through the membrane:[18]

- Grotthus mechanism: protons jump from one proton donor to a proton acceptor. They combine with water to form hydronium ion (H_3O^+), so protons move from one hydronium ion to another.
- Vehicular mechanism: water becomes the protons carrier, they mix with water molecules and hydronium ions pass through by electro-osmotic drag, following the water flow and proton movement from anode to cathode.

Grotthus mechanism is usually the dominant one, it is the fastest proton conduction mechanism in NFSA membranes, but the vehicular mechanism is the dominant one at low water contents.[21]

There are two major phenomena that should be taken into account to characterize the PEM electroyzer, they are the electro-osmotic drag and the permeation. They are gas or water crossover mechanisms that have a negative impact on cell performance.

Electro-Osmotic Drag

The electro-osmotic drag is a phenomenon that happens in proton exchange membranes, it is the movement of water through the membrane when it is dragged with the proton movement. The water molecules move from the anode to the cathode, mixing with the H_2 produced and reducing its purity. This can also cause problems with the hydrogen compressor after the electrolyzer, and it can provoke unwanted reactions. [4] [20]

The amount of water molecules transported by electro-osmotic drag depends on the current density, and it is proportional to temperature. It can be calculated by knowing the drag coefficient (n_{drag}) and applying the Faraday equation: [20]

$$J_{H_2O,Eod} = n_{drag} \cdot \frac{n_{cell} \cdot j}{4 \cdot F} \tag{4.15}$$

Where $J_{H_2O,Eod}$ is the electro-osmotic drag water flux, n_{cell} is the number of cells, j is the current density and F is the Faraday constant.
To calculate the total amount of water discharged, the water transported by diffusion must also be taken into account. The total water transported would be the sum of the electro-osmotic drag water flux and the diffusion water flux.

Permeation

Permeation is the process of gas crossover through the membrane. O_2 gas permeates from the anode to the cathode, and H_2 permeates from the cathode to the anode. This phenomenon

decreases the efficiency of electrolyzer and the gas purity, it is more noticeable when operating at high pressures.

For permeation to occur the gas must be dissolved, either in the water or the membrane. However, diffusion through the membrane in Nafion membranes is usually neglected, since it is very slow and the diffusion through the liquid water is considered the dominant mechanism of permeation. There are two mechanism which contribute to permeation: [4][22]

- Diffusion: H_2 and O_2 permeate from one side of the electrolyzer to the other due to the concentration gradient. Molecules travel from the side with higher concentration to the side with lower concentration. The diffusion flow rate of substance x ($J_{diff,x}$) can be calculated applying the Fick's law by knowing the diffusion coefficient (D_x^{eff}) of the substance "x", the difference in concentration from anode to cathode ΔC_x, and the membrane thickness (t_{mem}), which is the distance the substance has to travel: [22]

$$J_{diff,x} = D_x^{eff} \cdot \frac{\Delta C_x}{t_{mem}} \tag{4.16}$$

- Convection: dissolved H_2 and O_2 permeate from one side of the electrolyzer to the other due to electro-osmotic drag or pressure differences. They can permeate dissolved in water when water travels through the membrane as a result of the electro-osmotic drag, the convection flux can be calculated as: [22]

$$J_{con,x} = v_{H_2O} \cdot C_x = J_{\Delta P,x} + J_{eod,x} \tag{4.17}$$

  Where J_{con} is the convective flux of substance x, v_{H_2O} is the water velocity through the membrane and C_x is the concentration of specie x in water. Two different transport mechanisms comprise convection. The first one is the convection due to the pressure difference:

$$J_{\Delta P,x} = D_{\Delta P,x} \cdot \frac{P_x \cdot \Delta P}{t_{mem}} \tag{4.18}$$

  Where $J_{\Delta P,x}$ is the flux due to pressure difference, $D_{\Delta P,x}$ is the transport coefficient, P_x is the partial pressure of specie x in the part of the electrolyzer with higher presence and ΔP is the pressure difference.
  The second one is the convection due to the electro-osmotic drag:

$$J_{eod,x} = D_{drag,x} \cdot P_x \cdot j \tag{4.19}$$

  Being $J_{drag,x}$ the drag flux of specie x, $D_{drag,x}$ the drag coefficient, P_x the partial pressure of specie x in the part of the electrolyzer with lower presence, and j is the current density.

The total permeation can be calculated as the sum of diffusion and convective permeation. Gas crossover plays an important role in the design of electrolyzers, as high values of hydrogen crossover can originate instability and provoke explosions. [4]

4.3.5 Cathode Catalyst Layer

The cathode catalyst layer has the same purpose as the anode catalyst layer, but this one is used to stimulate the HER. Pt has always been used as catalyst, with a low catalyst loading, around 0.4-0.8 mg/cm^2.

To make the catalyst more accessible to large scale demands, platinum catalysts with carbon support have been developed, reducing the price of it. This is possible because of the non oxidizing conditions of the cathode. These catalysts present high catalytic activity, stability, conductivity, and performance. [4][23]

4.3.6 Gas Diffusion Layer

The gas diffusion layer is a kind of porous transport layer, but this one is situated in the cathode and receives the electrons from the PTL. Its goal is to perform a correct removal of H_2 gas in the cathode, preventing mass-transport limitations in the catalyst layer, or other inefficiencies like the blocking of active sites.

One of the biggest differences from the PTL anode is the material, the GDL is made of carbon based materials or even foam. This is possible because of the environment in the cathode is not acidic. Nevertheless, metallic materials have sparked interest due to their high conductivity and mechanical strength. [4] [6]

4.3.7 Operating Conditions

It is essential to operate at the optimum conditions in order to have the highest possible efficiency.

Temperature

Electrolyzers usually operate at high temperatures, since as a consequence of increasing temperature, the ionic conductivity of the membrane raises. Moreover, the activation potential decreases, increasing the exchange current density and improving performance. However, there are more cross currents at higher temperatures because of the random thermal movement of molecules, membrane relaxation, and increased gas permeability. The degradation has a faster effect at higher temperatures.[24]

The operating temperature is limited by the vaporization temperature of water, and also by the degradation and lifetime of the electrolyzer. The usual operation temperature is 60 to 80°C. [4][23]

Flow Rate

Another parameter that significantly affects the electrolyzer performance is the flow rate. It must be controlled to optimize the OER and HER, and to prevent mass transfer loss and degradation. Higher flow rates allow faster outgassing from the electrode surface and decreases mass transport losses.
The optimum flow rate varies depending on the characteristics of the electrolyzer, such as channel size and shape, PTL... So it is important to study each case specifically to know the maximum flow rate which gives the maximum current density possible. [23]

Pressure

Pressure is also an important factor in terms of electrolyzer efficiency, but it has a higher impact on the overall efficiency. Because hydrogen is stored at high pressure, it is worth

operating the electrolyzer at high pressures, to reduce mechanical compression and costs, and to increase the system efficiency.
There could be mass transport problems due to permeation when the cathode and anode are operated at different pressures, with a big pressure difference between them. At higher pressures, the hydrogen concentration in oxygen increases, so the electrolyzer must be operated at high current densities to not reach the dangerous level of 2% H_2 in O_2. [4][23]

The electrolyzer is usually operated at 1 to 30 bar, but it has been proven that it can be operated at 90 bar, producing high-pressure hydrogen without further treatments. [4][23]

4.4 Electrolyzer Characterization

4.4.1 I-V curve

The I-V curve or polarization curve is a plot of the cell voltage in relation to the current density. It is used to characterize the cell performance at different load conditions, providing information on performance loss. It represents all loss-mechanisms in the cell.
The cell voltage can be calculated using equation 4.3:[4][6]

$$V = V_{rev} + \eta_{act} + \eta_{ohm} + \eta_{conc} \tag{4.20}$$

Where V_{th} is the thermoneutral voltage, η_{act} is the activation overpotential, η_{ohm} is the ohmic overpotential and η_{conc} is the concentration overpotential

Figure 4.3 shows the polarization curve of an electrolyzer, with the thermoneutral voltage and the different overpotentials.

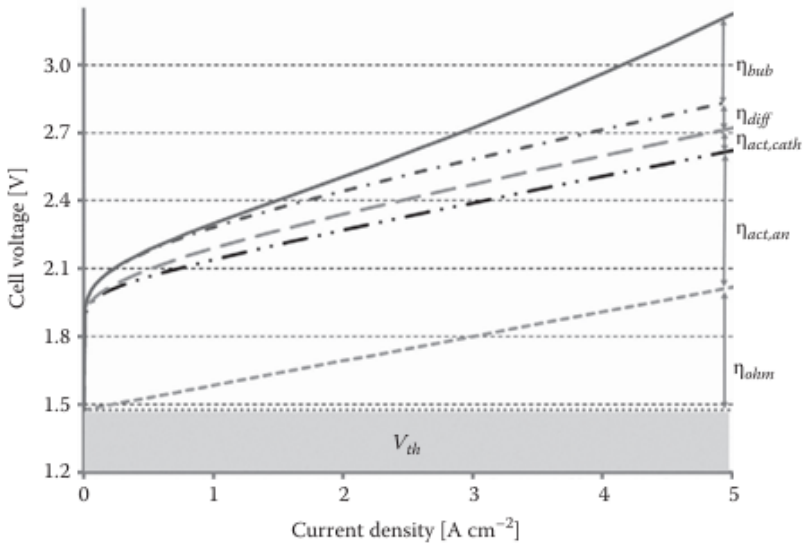

Figure 4.3. Electrolyzer I-V curve [4]

The polarization curve can be divided into three regions:[4][6]

- Activation region: corresponds to the activation overvoltage needed for the catalytic reaction. It is a exponential curve which takes place at very low current densities.

- Ohmic region: is the linear region in the middle, it is dominated by the ohmic overpotential. So, it is controlled by the electrical and ionic resistance of the membrane and cell components. The ohmic resistances are proportional to the membrane's thickness and inversely proportional to the membrane conductivity.

- Mass transport region: is the region at high current densities, dominated by the concentration overpotential. The voltage increases exponentially due to mass transport limitations.

The three overvoltage behaviors can be observed in figure 4.4, the activation overpotential has a huge impact at low current densities, the ohmic overpotential has a linear increasing impact, and the concentrations overpotential has an exponential impact at high current densities:

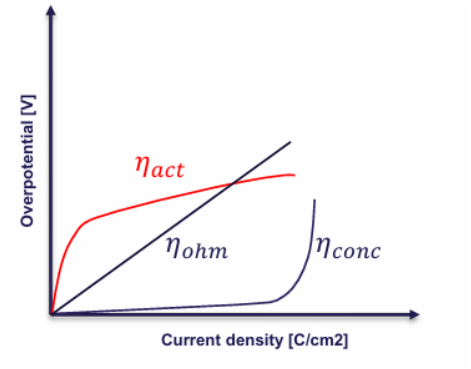

Figure 4.4. Overvoltages vs current density [25]

4.4.2 Efficiency

There are different electrolyzer efficiencies which can be measured:

- First law efficiency: it is the enthalpic efficiency, which takes into account the useful energy obtained (ΔH_{OR}) and the energy used or electric work (W_t).

$$\epsilon_{\Delta H} = \frac{\Delta H_{OR}}{W_t} \tag{4.21}$$

- Second law efficiency: relates the reversible electrical work (ΔG_{OR}) to the electrical work applied (W_t).

$$\epsilon_{\Delta G} = \frac{\Delta G_{OR}}{W_t} \tag{4.22}$$

- Voltage efficiency: relation between the ideal thermoneutral voltage (V_th) and the real voltage (V)

$$\epsilon_V = \frac{V_{th}}{V} \tag{4.23}$$

- Thermodynamic efficiency: relation between the reversible voltage (V_{max}) and the ideal thermoneutral voltage.

$$\epsilon_{th} = \frac{V_{max}}{V_{th}} \tag{4.24}$$

Faradaic efficiency is also important and it was described in section 4.2

4.4.3 Lifetime

Lifetime is the expected useful life of the electrolyzer, it is the time the electrolyzer can operate without changing core components or being stopped by a failure. It is approximated by knowing the degradation of the components. The proper selection of materials for the membrane and catalyst is crucial to improve the lifetime of the device. [4]

The lifetime can be stated depending on safety or economic conditions. The safety end of life condition for electrolyzers is usually the loss of thickness of the proton exchange membrane to 20% of the initial thickness. At this point, gas crossover would likely pass the safety limit of 2%.
Lifetime is also limited by the efficiency of the cell and the economic profitability it can offer. The catalysts play an important role here, since they degrade considerably over time, reducing the performance of the electrolyzer. They must be substituted when necessary. High loading of Pt increases the expected lifetime of the electrolyzer. [4]

Nowadays, electrolyzers can reach more than 60,000 hours of operation when they use high platinum loadings. [4]

4.5 Degradation Theory

Degradation plays a key role in the performance of PEM electrolyzers through time. It defines the end of life of the cell.

There exist a lot of different mechanisms that contribute to degradation. Figure 4.5 shows the most important degradation mechanisms and their impact on the cell performance.[4] [15]

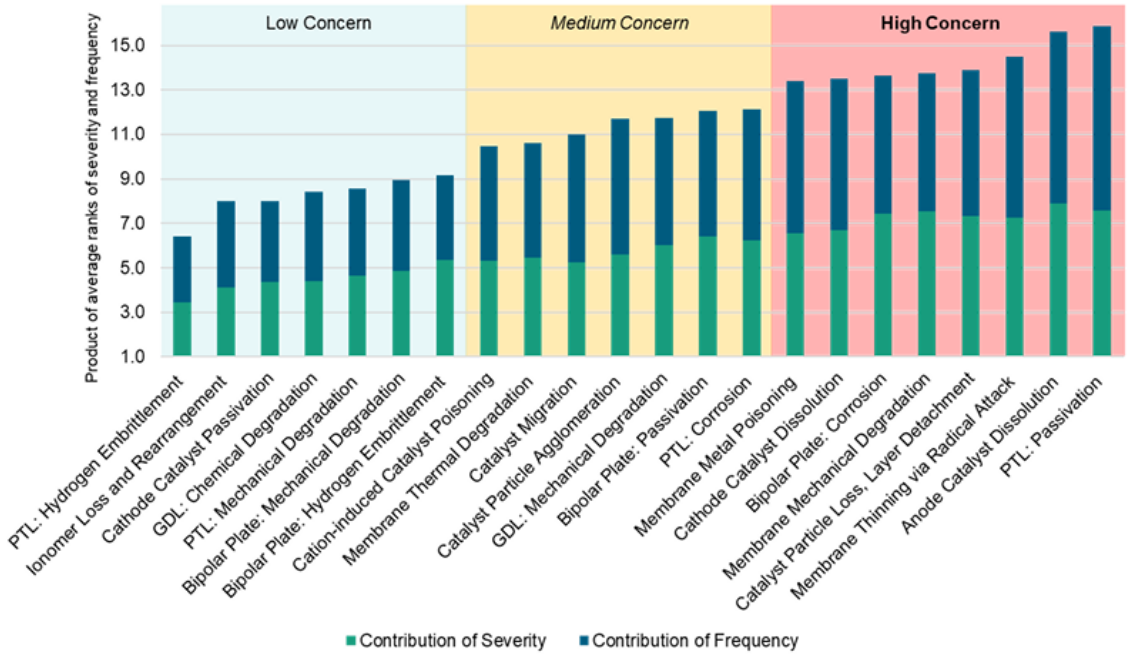

Figure 4.5. Degradation mechanisms [15]

These mechanisms can be divided into three groups, depending on the cause of the degradation, these are chemical, electrochemical, mechanical, and thermal. Most of the effects of degradation are irreversible, meaning that the cell will never reach its initial performance, this is one of the reasons why it is important to calculate the degradation from the very beginning. As can be seen in figure 4.5, there are a lot of degradation mechanisms in the operation of PEM electrolyzer, the most important ones are described below: [2]

4.5.1 Chemical Ionomer Degradation

The chemical ionomer degradation or membrane thickness via radical attack is the decrease in membrane thinning because of the attack of radical species which react with membrane molecules in the edge of the membrane. [17] [15].

Hydrogen peroxide radicals are produced from hydrogen oxidation, they can be produced at low potentials (0.682 V) in acidic environments in presence of oxygen and protons. This kind of degradation can occur either from the anode and from the cathode. However, it mostly takes place on the anode side due to the higher presence of oxygen. It is also enhanced at low current densities; the lower the potential, the higher the stability of radicals.
Then, these radicals react in a complex reaction mechanism, consuming the end groups of the membrane and releasing fluoride. This is why the fluoride release rate is used to estimate

the degradation rate. [17]

Contaminated environments stimulate this kind of degradation, e.g. metallic traces in the input water, such us Fe^{+2}, can react to enhance the formation of radicals which react with the membrane.

The chemical ionomer degradation of the PEM has many different effects to consider on the cell performance. The most remarkable ones are the releasing of unwanted substances, the increment in membrane resistance and gas crossover, the change in membrane structure and water uptake properties, the formation of pinholes in the membrane, local temperature peaks, and the decrease in mechanical properties. [17]

The main strategies to prevent the chemical ionomer degradation are:

- Using optimized operating strategies and energy buffer management to reduce the time spent on idle load and during rapid load changes, which can cause voltage spikes and drops.
- Do not have contaminants in the water input.
- Well humidified membrane, moderate temperatures and low hydrogen pressures.
- Uniform distribution of temperature and humidification by having a correct flow field design given by membrane components such us GDL.

4.5.2 Ionomer Inhibition

The ionomer inhibition is the loss or reduction of proton conduction in the membrane, it is the blocking of the functional sulphonic end groups of the ionomer. It is caused by the ion change of Brønsted acid sites with cations due to contaminants. The contaminant which affects ionomer inhibition the most is the NH_4^+ that comes from NH_4 or NO_x compounds reduced with hydrogen. [17]

These inhibition originates an increment in membrane resistance due to the blocking of functional groups for the proton transport. It also modifies the water uptake behaviour and its conductivity as well.[17]

It can be mitigated by avoiding the impurities which contribute to the ionomer inhibition, using additives and auxiliary materials, and by avoiding bipolar plates degradation and corrosion. [17]

4.5.3 Passivation

Passivation is the formation of an insulating oxide layer in the surface of metal materials. It can occur in any component with metallic components, such as bipolar plates, PTL or catalyst layers. It is more noticeable in the bipolar plates. However, PTL passivation has the highest impact on cell degradation.[15]

Passivation increases the contact resistance, which decreases the interfacial contact, reducing the electric conductivity or catalyst detachment between the PTL and CL. It has a higher impact on the anode side. [4]

4.5.4 Mechanical Membrane Degradation

The membrane is usually deformed with time when the electrolyzer is operating, it decreases its performance. There are different factor that affect the membrane deformation, such as the chemical degradation, physical stresses, high operating temperatures, swelling and shrinking of the membrane, and the reduction of humidity level. [17]

This kind of degradation decreases the proton conductivity of the membrane, it increases the gas permeation, voltage losses, current reversal, provokes local temperature peaks.
It can be mitigated by controlling the membrane humidity, by avoiding dry-out, pressure differences and overpressures, by using thicker GDL, by reinforcing the membrane... [17]

4.5.5 Platinum Catalyst Degradation

There are three main mechanisms that contribute to platinum degradation:[17]

- Dissolution and redeposition: an electrochemical platinum dissolution can be possible at potentials below 1.188V in acidic environments. It is also oxidized at potential higher than 0.98V, and then platinum oxide can be dissolved with hydrogen protons. Platinum can also be dissolved with chlorides.
  Particle growth also occurs by Ostwald ripening, by coalescence with platinum dissolution, or by migration. This phenomenon increases the particle size of platinum, so fewer and larger particles stay in the catalyst layer, providing less activation surface for reactions to happen.

- Detachment and coalescence: it occurs due to particle growth, carbon support degradation, mechanical impacts or weak bonding to the carbon surface support.

- Poisoning and blocking: poisoning happens when the catalyst adsorbs compounds that block the active surface of the catalyst. There are different substances that poison the catalyst, such as CO, NO_2, H_2S...

These platinum degradation mechanisms usually cause an irreversible catalyst surface deactivation, decreasing the catalyst performance and increasing the overvoltages needed. It can also cause the formation of a platinum band, which is the redeposition of platinum particles inside the membrane. [2]

Some strategies to prevent or mitigate catalyst degradation are the avoidance of high cell voltages, highly transient operation, cell reversal, start/stop operation, high temperatures, wrong catalyst distribution, not optimal humidity and contaminants. [17]

4.5.6 Iridium Catalyst Degradation

Iridium catalysts are very stable and resistant to corrosion, but can be electrochemically dissolved at high potentials. Soluble iridium oxide is formed by hydrolysis at potentials higher than 2.1V. Chlorine ions can also cause chemical dissolution. [2]

As for platinum catalyst degradation, the iridium also suffers particle growth by Ostwald

ripening, coalescence, and migration. The active surface is poisoned by contaminants and metal ions. Iridium catalyst is subjected to more mechanical stresses due to the gas bubbles in the anode, provoking more detachment. The iridium catalyst degradation is also mostly irreversible. [2]

The causes, effects, and strategies to avoid iridium catalyst degradation are very similar to those mentioned for the platinum catalyst

4.5.7 Carbon corrosion

Carbon-based materials can suffer corrosion when operating at high potentials. Under acidic conditions, carbon is only stable under 0.207V. At higher potentials, reaction (4.25) starts to occur, and solid carbon is consumed by reacting with water.[17]

$$C_s + 2H_2O \rightarrow CO_2 + 4H^+ + 4e^- \tag{4.25}$$

Carbon corrosion causes the thinning of carbon-based layer, it increases ohmic and contact resistances, and decreases the electrolyzer efficiency. Some mitigation strategies are: [17]

- Adding platinum particles: they lower the kinetic oxidation resistance and make the cell operation more stable.

- Operation conditions: avoid low current densities, very high cell voltage, and transient operation.

4.5.8 Reversible Degradation

Reversible degradation is the kind of degradation that causes losses which can be recovered or, at least, partly recovered. A change in the electrolyzer operation conditions or a operation stop is usually enough to reverse the degradation.

Some reversible degradation factors are catalyst restructuring, contamination, water management, and ionomer degradation. The low anode loading, high current density, inhomogeneous anode coatings, and low operating conditions stimulate the increase in reversible losses. Strategies have been developed to minimize this losses. [26]

Reversible degradation is more noticeable at high current densities. The factor that affects the most to reversible degradation is the creation of oxygen bubbles that can get stuck inside the electrolyzer and decrease the mass transport efficiency.
An electrolyzer shutdown is usually enough to recover most of the degradation.[27]

Experiment Description 5

This chapter describes the theory behind the experiment and the tools and components used to carry it out.

The experiment is carried out on a device called Innovation Greenlight electrolyzer test equipment. This is a device developed by the company named Greenlight Innovation, it consists of a station designed to easily control all the operation conditions. A DC regulated power supply is attached to the station to supply electricity.
It also comes with software which allows to control and set up the operation parameters, storage and display data, control the process...[28]

5.1 Electrolyzer components

The electrolyzer components used for the experiment are described in this section. Figure 5.5 shows how the electrolyzer looks after being assembled:

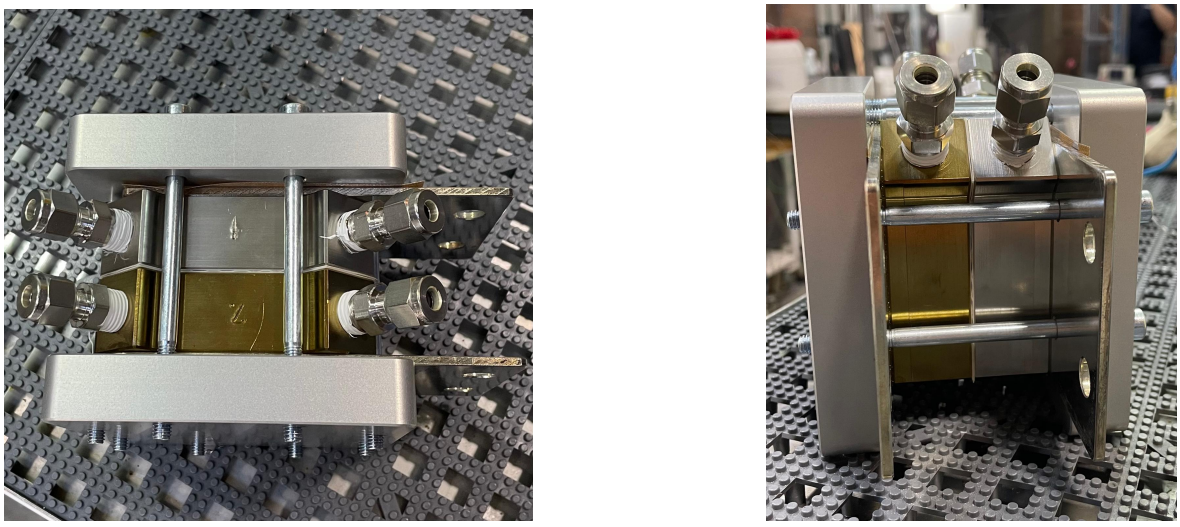

(a) Electrolyzer top view ***(b)*** Electrolzer front view

Figure 5.1. Electrolyzer top view (a) and front view (b)

5.1.1 Membrane

The membrane is made of Nafion117, with a thickness of 183 μm. It has an anode and cathode side coated with ultrasonic spray deposition.
The anode catalyst is of type IrO_x, with a size of 2-5 nm and a weight percentage content of

Ir of 17.35 ± 1.14%. The catalyst loading in the anode is 0.5 mg/cm^2, and it is uniformly distributed.

The cathode catalyst is of type Pt/C, with a weight percentage content of 47.1%, The cathode catalyst loading is 0.3 mg/cm^2, and the size is unknown.

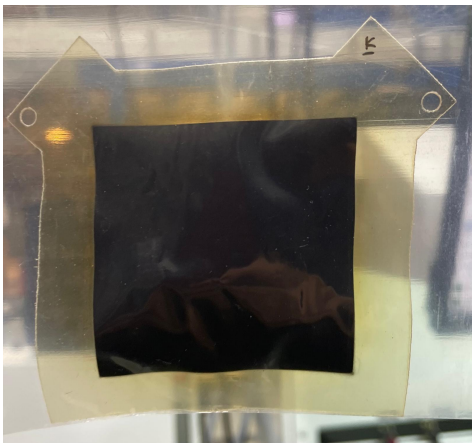

Figure 5.2. Membrane used for the experiment

5.1.2 PTL

The PTL is 5x5 cm layer made of Ti and coated with Pt to mitigate degradation. It has a thickness of 0.51 mm and a porosity of 56%. [29]

5.1.3 GDL

The GDL is made of Toray carbon paper 060, which is a carbon fiber paper. It has a thickness of 190 μm and a standard 5% weight wet proofing. Later in the experiment, these GDL will be changed for a new one with a thickness of 280 μm. [30]

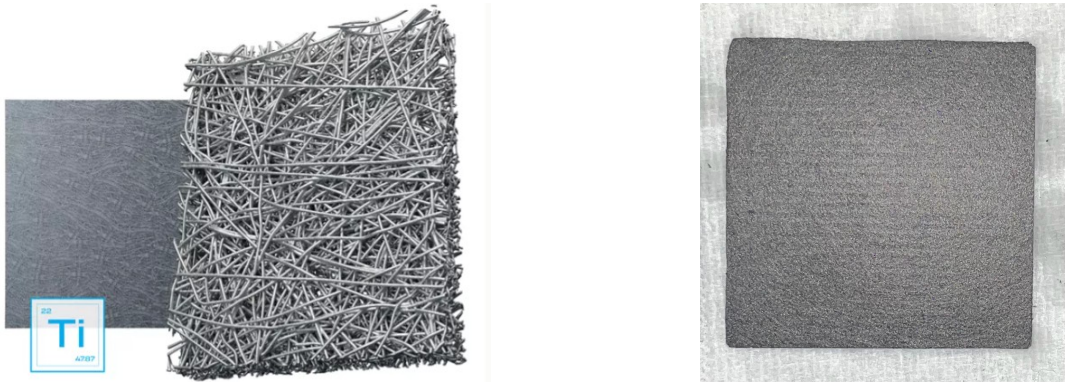

(a) PTL and its structure [29] ***(b)*** GDL

Figure 5.3. PTL (a) and GDL (b)

5.1.4 Flow Plates

Flow plates are titanium blocks which have holes and flow fields on them, they are coated with a passivation layer to prevent corrosion. A heat treatment process must be done before usage to prevent leakage. The electrolyzer needs two of these blocks, one for the anode and

the other for the cathode.
The one in the anode is coated with Pt and it is planned to have water as input and output. The one in the cathode is coated with Au and is planned to have only hydrogen output. Figure 5.4 shows the anode plate and its flow distribution pattern. The same pattern is used for the cathode.

Figure 5.4. Flow plate. Photo courtesy of Hamilton Delaney

5.1.5 Gaskets

The gaskets are used to prevent water and hydrogen leaking and electrical short circuits. It is a layer of PTFE that is fitted inside the flow plates and around the GDL and PTL. Two kinds of gasket are used during the experiment, one with a thickness of 0.5 mm and other with a thickness of 0.25mm. Figure 5.5b shows an image of the gaskets used.

5.1.6 Current Collectors

Current collectors are in charge of receiving electricity and distributing it through the electrolyzer. They are 127x76.2mm 99.95% pure Cu blocks with holes to make assembly easier. They are coated with a Tin layer to prevent corrosion.

(a) Current collector

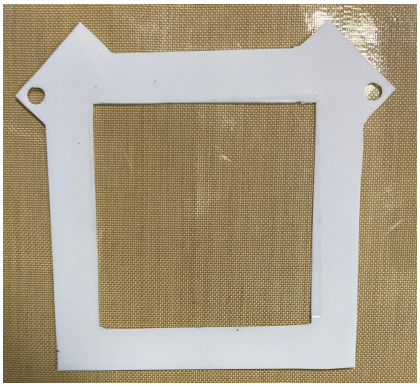

(b) Gaskets

Figure 5.5. Current collector, photo courtesy of Hamilton Delaney (a), and gasket (b)

5.2 Break in/Conditioning

The process called break in or conditioning of the PEM electrolyzer is needed to ensure the correct and optimum operation of the device from the beginning.
The most noticeable benefits are the removal of impurities in the membrane electrode assembly, the activation of catalysts, the creation of pathways from reactant to catalyst, and the hydration of the membrane and catalyst layer, which leads to better proton transfer efficiency.[31] [32]

There are different ways to carry out this process, depending on the operating conditions. One accepted process can be done following the next steps: [31] [32]

1. The cell is warmed up to the desired temperature by using the water which goes through it.
2. When the desired temperature is reached, a current density of 0.2 $A \cdot cm^2$ is applied for 30 minutes.
3. The current density is increased to 1 $A \cdot cm^2$ for another 30 minutes.
4. The cell is operated at a constant voltage of 1.7 V until the current is stabilized, with current variations lower than 1% per hour.
5. Data points are registered every period of time to obtain performance curves and verify the process.

The time needed for the conditioning process varies depending on the operating condition, e.g., up to 12 hours at 60 °C and lower time at 80 °C. There is no universal method that works better than another in all situations. That is why it is important to record the cell stability, and repeat the polarization curve measurement at least 3 times.

There exist faster methods of conditioning than the one presented before, but it has been found that slow conditioning processes are better in terms of electrolyzer performance and prediction. Since the OER kinetics improve, the high-frequency resistance and the electrode capacitance increase, and the polarization curve hysteresis decreases.[33]

5.3 Data measured

The data taken from this experiment are directly recorded by the Greenlight fuel cell and electrolyzer test equipment and its software. Data are taken every 3-4 days. I-V curves are obtained by manipulating the current of the system. The current is set at 0A and is increased to 50A with a step of 1.25A, in each step the voltage production is written down after waiting for the system to stabilize. Hydrogen production is also recorded in each step.

After one week and a half of the experiment, an automatization code was made to collect the data for the IV. This code essentially performs the same procedure mentioned above, but it does it automatically, stopping 60 seconds between current steps.

In the results and discussion section, the data are presented with the dates in which they were taken. Not all data plots are presented, only the most relevant ones.

Different kinds of data can be obtained depending on what is interesting to analyze, i.e. data varying only the water recirculation flow is also taken during the experiment or EIS. However, another data measuring device is needed to calculate the resistances inside the electrolyzer by doing an electrochemical impedance spectroscopy (EIS). A device called Reference 3000 Potentiostat produced by Gamry Instruments is used for this purpose. EIS measurement is performed during the electrolyzer operation. [34]

5.3.1 EIS

EIS is a technique used to analyze the performance and resistances of the electrolyzer by examining the internal chemistry that happens inside the device, obtaining real-time information of electrode processes, polarization process, and reaction kinetics. It consists of measuring electrical fluctuations provoked by applying sinusoidal signals and perturbing frequencies in a small range. [35] [36] [37]

An equivalent circuit model is established using the EIS, then information such as ohmic resistance, double layer capacitance, and charge transfer resistance can be extracted. EIS is performed to obtained two different plots which give important information about the electrolyzer: [37] [38]

- Nyquist plot: it shows the correlation between the real and imaginary impedances when the frequency varies. The frequency information is not directly represented as an axis of the plot. Identification processes are performed to identify the different kinds of resistance using the Nyquist plot, i.e. a 45° line at low frequencies means mass transport resistances, semicircles are found in the medium frequency range and they correspond to charge transfer or chemical resistances. Figure 5.6 shows a typical Nyquist plot for an electrolyzer, differentiating between the different zones. On the one hand, the OER is the slower and rate limiting process, so the anode activation losses are represented at low frequencies. On the other hand, the cathode activation losses are represented at higher frequencies, since the HER is faster. [37] [38]

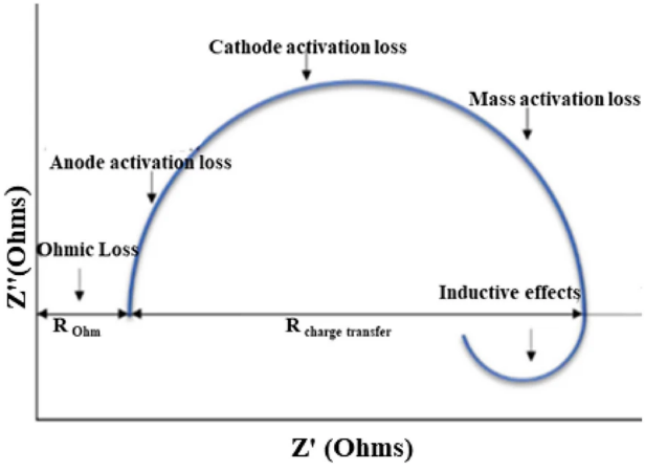

Figure 5.6. Typical Nyquist plot[39]

- Bode plot: it is a different way of representing the same information as the Nyquist plot, but with a direct relation to frequency. The magnitude and phase angle of the impedance are plotted as a function of the frequency in the Bode plot. The impedance magnitude is represented on the left side X-axis, and the phase angle in the right side X-axis.
  Drops in frequency represent charge transfer or chemical resistances, and flat regions at high frequencies represent ohmic resistances. Another important aspect is that the number of peaks in the phase angle plot equals the number of resistor-capacitor equivalent circuits (RC). An ideal Bode plot of a parallel RC circuit is presented in figure 5.7. At low frequencies, the resistor dominates, maintaining constant impedance and a 0° phase angle. At high frequencies, the capacitor short circuits the resistance, causing the impedance to decrease linearly and the phase angle to approach 90°. [37] [38]

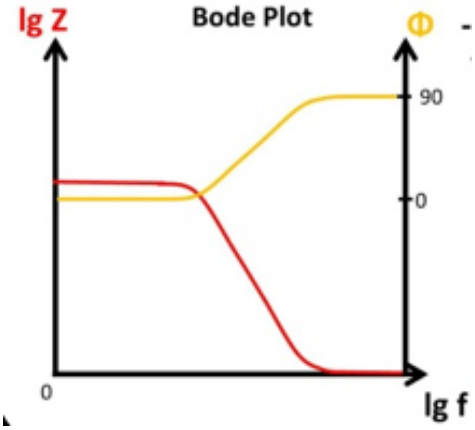

Figure 5.7. Ideal Bode plot [40]

Experiment Procedure 6

The procedure to carry out this experiment can be described following the next steps:

1. Cell assembly
2. Cell pretreatment
3. Leaking test
4. Initial test
5. Break in
6. Electrolyzer operation
7. Data analysis

To obtain a clearer vision of the procedure, figure 6.1 shows a process flow diagram of the procedure applied:

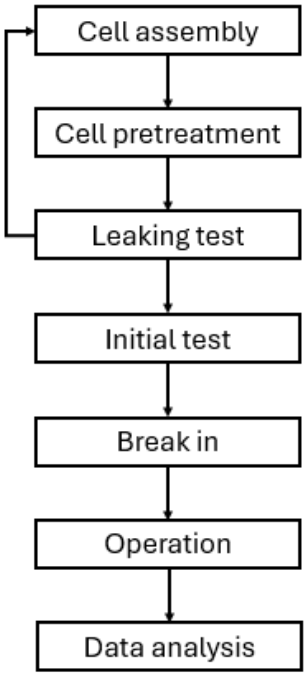

Figure 6.1. Procedure PFD

6.1 Cell assembly

Cell assembly was done after all the required components were obtained, and modified in size, if needed. 3 GDL layers were used in the cell to match the thickness of the PTL and ensure correct cell operation. So, a total of 570μm was reached. However, these three layers

would be changed later in the experiment for a single GDL with a thickness of 280μm.
Plastic pins must be used to connect all the components. At first, metal pins were used, but this originated a problem in the cell, since the electricity flowed through these metal pins instead of following the desired path.

After properly connecting all the electrolyzer components, they are torqued together following manufacturer's procedure. Following a star pattern, all bolts were tightened in increments: first to 10 in·lbs, then 20, 30, and finally to 40 in·lbs.

6.2 Cell pretreatment

The cell can be subjected to a thermal pretreatment to try to prevent assembly problems such as leaks. The membrane electrode assembly can be introduced in an oven at 140°C for 2 hours. At higher temperatures, the cell materials become more flexible and the curvature of cell and assembly imperfections can be corrected.
The pretreatment can also be a mechanical pretreatment, but the thermal one presents more advantages.

In this experiment, only the gaskets are pretreated in the oven, with the purpose of removing the curvature and preventing possible leaks.

6.3 Leaking test

The leaking test is performed to check if there is any leakage and if so, fix it.
Air is introduced on the anode side of the cell, then the pressure is maintained constant at low values, the valve of air input is closed, and if the pressure drops, it means there is a leakage. In this case, a leakage detector fluid is used to identify the location of the leak. It is applied in the possible locations, such as bonds or connections, and if the creation of air bubbles is observed, it means that the leak is there. Finally, the cell is modified to fix that leak, it can be modified by tightening the bolts or by other methods.

The same procedure is repeated until there are no leaks, then it is carried out in the cathode side.

6.4 Initial test

An initial test was performed to verify the proper functioning of the electrolyzer. This test consists of obtaining the I-V curve of the cell for a current density from 0 to 2 A/cm^2.

The operation conditions are written down, and the current is increased from 0 A to the value needed to obtain a current density of 2 A/cm^2, in this case this value is 50 A, since the area is 25 cm^2. The current is increased by 2.5 A for each data-point and the values of voltage are written down. Additionally, the values of hydrogen produced flow were also noted.

6.5 Break in/Conditioning

It was decided to do the break in by operating the cell at 80°C, 0.5 A/cm^2 and 0.5 NLPM of recirculated water for 48 hours, and then increasing the current density to 1 A/cm^2 for 24 hours, following the European standard. [41]

6.6 Electrolyzer operation

After the break in is conducted, the electrolyzer is ready to start normal operation. The operation conditions are selected and established for the experiment. The experiment is supposed to run for 6 consecutive weeks, reaching over 1000 hours of operation.

The conditions selected for this experiment are a temperature of 80°C and a pressure of 1 atm. These conditions are widely used when testing the PEM electrolyzer degradation, making easier the comparison with literature.

At higher temperatures, the PEMEL increases its efficiency, and more hydrogen is produced, but the degradation also increases. So, when operating at 80°C for the established period, significant degradation will be observed and can be studied.

It is operated at 1 atm for safety reasons, and to make the comparison easier. It also allows to study different kinds of degradation, at lower pressure, less mechanical degradation, and more chemical, thermal, and reversible degradation would be observed.

The cell is operated at a current density of 2 A/cm^2. This condition increases the production of hydrogen and the degradation, making it suitable for the purpose of the experiment.

The water conductivity must be less than 0.3 μS/cm to consider the water as DI water.

6.7 Data analysis

Data are taken during the experiment, and they are processed to obtain a visual representation of what is happening in the electrolyzer and to reach conclusions.

The results are discussed while the experiment is still running in order to optimize conditions and solve possible issues that can affect the electrolyzer performance.

Results and Discussion 7

The data obtained from the experiment are presented and discussed in this chapter. This chapter is divided into initial test, first experiment, and second experiment. Data were taken periodically every 3 to 4 days. However, only relevant plots will be presented in this section. In addition, one last experiment in which degradation is very remarkable is presented. Finally, results obtained from a simulation model are presented to gain a clearer vision of the results.

The results were decided to be expressed making a distinction between the two different electrolyzer assemblies, this is because of the significant efficiency difference between them and possible variations in degradation effect. The first experiment corresponds to the electrolyzer operation using 3 GDLs of 0.19mm thickness each. The second corresponds to the operation with one 0.28mm thick GDL.

An electrical short circuit was present throughout all the experiments, but it was identified and fixed on 9th of December. However, it was too late to obtain relevant data for the project. So, a small section dedicated to the data obtained for the healthy electrolyzer setup is presented.

To obtain a clearer vision of the actions performed that could affect the electrolyzer proper function, a chronological enumeration is made up as overview:

- Disassembly to change gaskets.
- Disassemblies to fix leaking problems.
- Disassembly to change metal pins for plastic pins.
- Disassemblies to add the three GDLs.
- Disassembly to change the three GDLs for a single one.
- Disassembly to change GDL dimensions and measure ohmic resistance of the different parts of the electrolyzer. The membrane was completely dried during this process

Isolating the electrolyzer by wrapping it with a thermal isolating material would be very beneficial for the purpose of the experiment, since the temperature is unstable through the electrolyzer operation.

7.1 Initial test

The initial test was carried out with a water flow of 0.25 L/min and an initial temperature of 71°C, which rose up to 73°C during the experimental period. This temperature instability was considered to not affect negatively to the purpose of the initial test.

O_2 was present in small quantities during the entire experiment period. There was O_2 even when there was no production of H_2, this could be due to the previous operation of the electrolyzer before starting the experiment. A measurement problem of the station was considered to be the reason of the wrong oxygen output number, it was considered to not have a negatively effect on the electrolyzer operation. The whole experiment was carried out ignoring this output variable.
Figure 7.1 shows the IV curve obtained from the initial test. It can be observed how the voltage increases linearly with the current density until the thermoneutral potential is reached. Then, the voltage also increases linearly following the ohmic resistances.

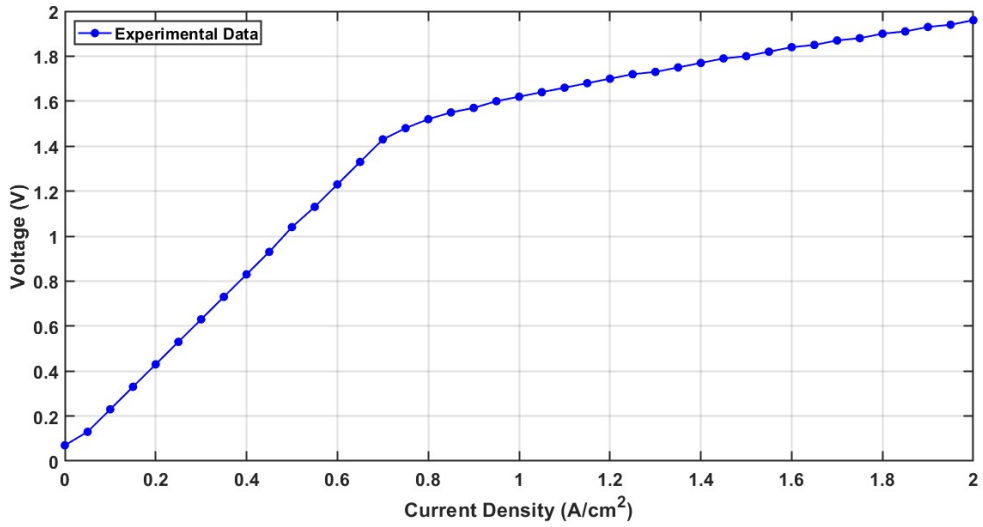

Figure 7.1. 1st test polarization curve

Figure 7.2 represents the hydrogen produced, in normal liters per minute, at different current densities. It can be observed how there is no hydrogen production until the current density is 0.75A/cm^2, the thermoneutral voltage of 1.48V is reached, and reactions start to occur. Then, the hydrogen production increases linearly, following the Faraday's Law.

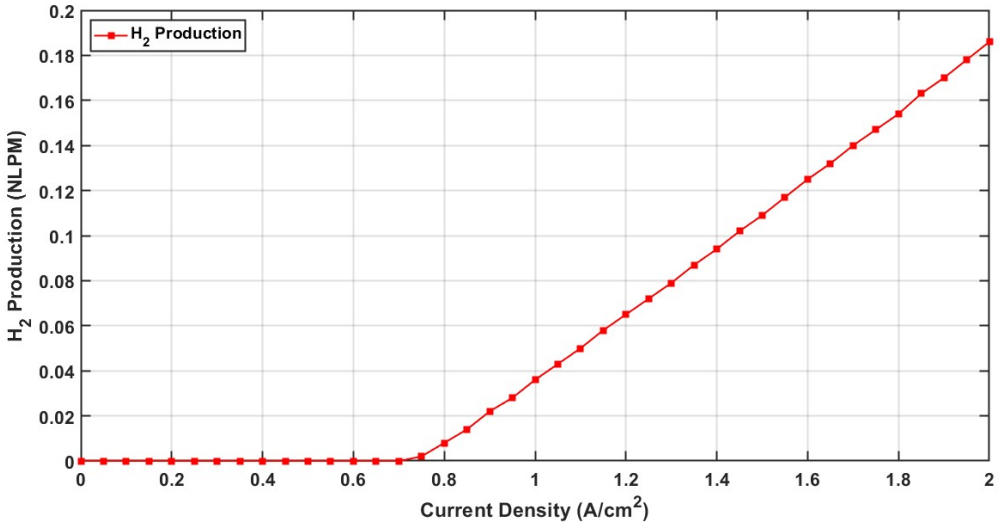

Figure 7.2. 1st test hydrogen production

The initial test shows two main problems, a higher voltage than expected and the wrong

behavior of the IV curve. To fix the overvoltage problem, more GDLs were assembled in the electrolyzer, trying to avoid ohmic resistances, the PTL thickness was taken as a reference for the proper functioning. After adding a second GDL, the experiment officially began. The problem regarding the IV curve will be approached in the next sections.

7.2 First experiment

7.2.1 Test 1

The experiment began on October 30th at 10:00 AM. Figure 7.3 shows the IV obtained at 76°C.

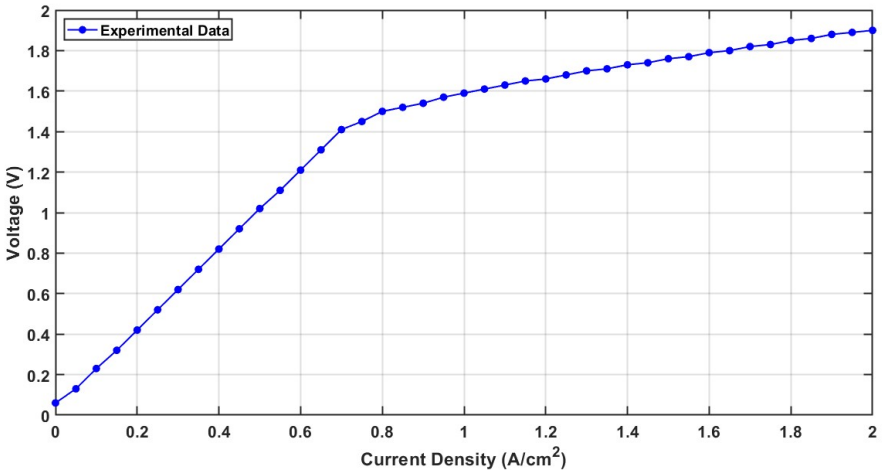

Figure 7.3. I-V curve at 76°C (30/10/2025)

To try to fix the still present problems, the electrolyzer was disassembled and a new GDL is added to the cell, having a total of 3 GDLs. The total thickness of the GDL is now 0.57mm which is larger than the gasket thickness, and the PTL thickness is 0.51mm. The gaskets also play an important role here, since if the gasket is much thicker than the GDL or PTL, it could cause a contact inefficiency between layers, increasing the ohmic resistance and decreasing the electrolyzer performance.

7.2.2 Test 2

The second I-V curve was measured on the 4th of November. The result is shown in figure 7.4, an improvement in performance can be observed, voltage drops from 1.9 to 1.83V at 2 A/cm^2. The electrolyzer temperature is 78.5°C, which also plays a role in the increase of the voltage difference:

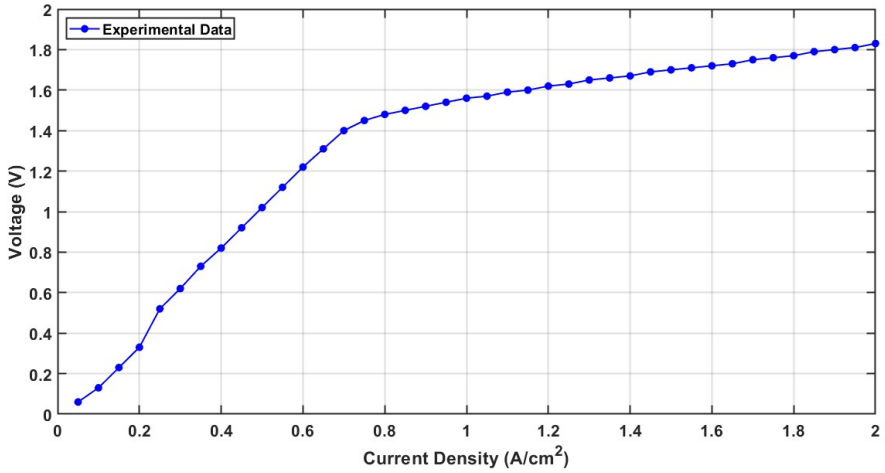

Figure 7.4. I-V curve at 78.5°C (04/11/2025)

When comparing this figure to literature, a big difference can be observed, the voltage starts at 0V and increases linearly. Literature shows curves that start at the Nernst potential value, which would be around 1.23V for this case. [4] [42].
This difference means there is something wrong with the equipment or the cell, it is not working as intended.

When comparing the IV curves obtained to the ones provided by the manufacturers, it can be observed how the experimental IV curves are shifted 0.7 A/cm^2 to the right for the 1st experiment. To identify this problem, the electrical resistance between the anode and cathode was measured, obtaining a very low result.
This could mean that there is a soft short between the anode and the cathode, or that there is an unwanted resistance in the cell, caused by a leak, or an assembly or component problem.

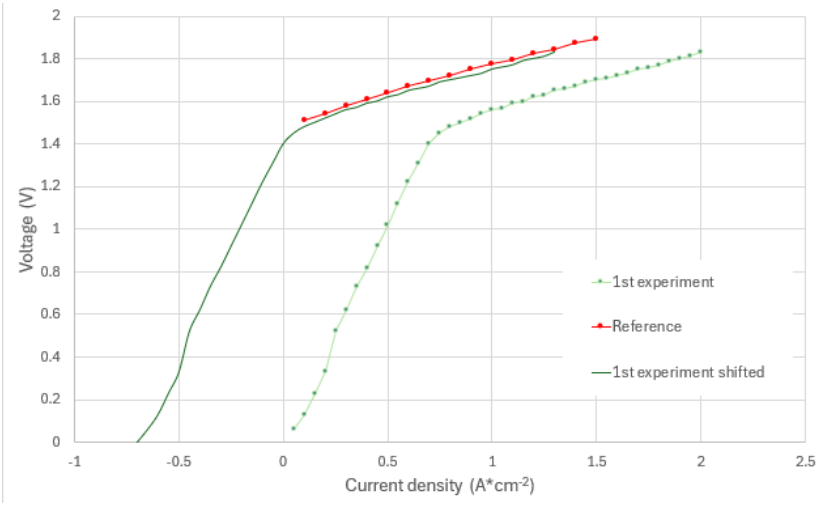

Figure 7.5. Comparison with manufacturer

The line does not exactly overlap the manufacturer's curve because differences in the electrolyzer or operation conditions, i.e. the IV curve obtained experimentally was measured at 78.5°C, and the manufacturer's at 75°C.

A mathematical validation was also performed to check the results. The amount of hydrogen produced is calculated applying the Faraday's law and it is then compared to the experimental values obtained. The hydrogen produced is shown in figure 7.6:

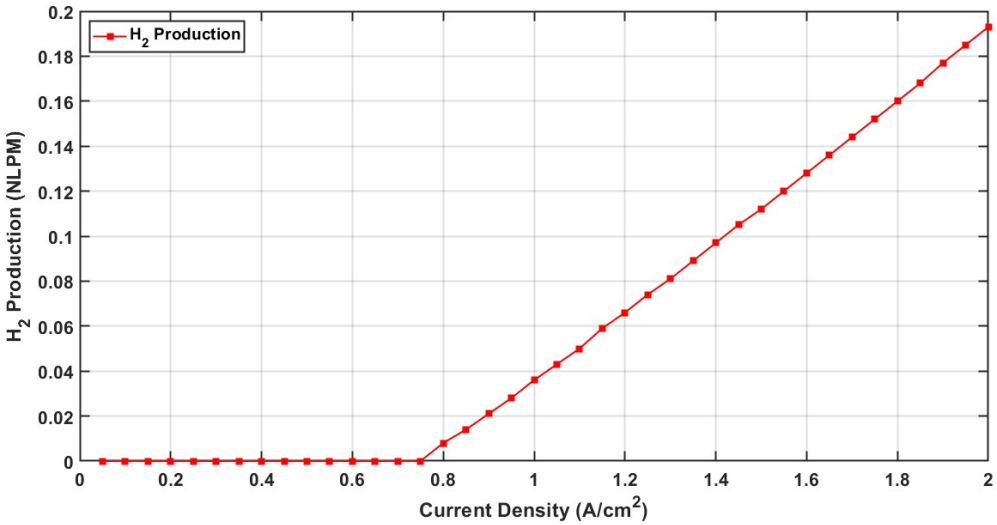

Figure 7.6. H_2 production 04/11/2025

The mathematical value obtained for a current density of 1 A/cm^2 and assuming a Faradaic efficiency of 100%, is $2.61 \cdot 10^{-4}$. However the value obtained experimentally is $5.4 \cdot 10^{-5}$ g/s.

Another comparison was done for a current density of 1.5 A/cm^2. The mathematical value obtained is $3.92 \cdot 10^{-4}$ g/s, and the experimental value is $1.68 \cdot 10^{-4}$ g/s.
For a current density of 2 A/cm^2, the mathematical value is $5.22 \cdot 10^{-4}$ g/s and the experimental one is $2.90 \cdot 10^{-4}$ g/s.

We can observe how the mathematical and experimental results differ significantly, with a higher difference at lower currents. At higher currents, the difference is reduced.
The Faradaic efficiency goes from 20.69% at 1 A/cm^2 to 55.55% at 2A/cm^2. The electrolyzer usually has a 98% or higher Faradaic efficiency.

Water recirculation flow

Another test was performed to investigate the effect of the water recirculation flow in the electrolyzer, since the inlet pressure in the anode was considerably high, about 4.40 barg. This condition causes a larger pressure difference in the electrolyzer, increasing convection and, as a consequence, degradation.

Table 7.1 shows the data taken at different flow rates of water recirculated, while the electrolyzer operates at 50A and 80°C. It can be noted how the voltage is maintained constant with a small increase, which has nothing to do with the recirculated water. The inlet pressure drops significantly without affecting the outlet pressure and hydrogen production. However, the temperature of operation decreases from 79.1 to 77.5 °C due to less hot water recirculation, which could cause some inefficiencies.

The performance of the electrolyzer was found to be not affected by pressure or water recirculation.

Table 7.1. H_2O recirculation influence

H_2O_{re}**(LPM)**	**C(A)**	**V(V)**	P_{in}**(barg)**	P_{out}**(barg)**	**T(ºC)**	H_2 **(NLPM)**
0.50	50	1.83	4.40	0.45	79.1	0.192
0.46	50	1.83	4.12	0.43	79.1	0.191
0.42	50	1.83	3.85	0.44	79.1	0.191
0.38	50	1.83	3.60	0.44	79.0	0.192
0.34	50	1.83	3.30	0.44	79.0	0.192
0.30	50	1.83	3.00	0.44	78.9	0.191
0.26	50	1.83	2.72	0.44	78.8	0.191
0.22	50	1.83	2.47	0.44	78.7	0.191
0.18	50	1.84	2.22	0.44	78.4	0.191
0.14	50	1.84	2.00	0.44	78.3	0.191
0.10	50	1.84	1.79	0.44	78.1	0.191
0.06	50	1.84	1.50	0.44	77.5	0.191

After proving that the recirculated water flow does not have a significant impact in the electrolyzer performance, it was decided to establish 0.25 LPM, 2A/cm^2 and 80°C as the definitive operation conditions.

A small increase in the voltage can also be observed after the established conditions are reached and some time passes, it increases from 1.82V to 1.84V. This happens because of operation initialization and reversible degradation.

When the electrolyzer first reaches 2A/cm^2 there is more energy loss in the form of heat, which stimulates the performance of the electrolyzer, and less voltage is needed. However, after some time in equilibrium, there are less energy losses, and the energy needed must be supplied applying a higher voltage. This is one of the reasons why the voltage is higher after some time in equilibrium. [43]

There is also a higher difference in species concentrations from anode to cathode, which causes an increment in the concentration overpotential. There are more resistances due to bubbles generated and stuck in the PTL or CL, which lead to more losses. This is a type of reversible degradation, it negatively affects the performance but can be reversed. [44]

7.2.3 Test 3

It was decided to continue with the electrolyzer operation while trying to fix the overvoltage problem. An EIS test was performed on 7th November to try to identify the resistances in the electrolyzer. As it could be expected, they do not correspond to the ones presented in the literature.
3 EIS test were carried out to validate the results, all tests give practically the same result. Results are presented taking into account all the frequencies, figure 7.7a, and avoiding frequencies lower than 10 Hz, figure 7.7b. Low frequencies are usually not represented in the Nyquist plot due to the instabilities of the system during the measurement, like bubbles movement.

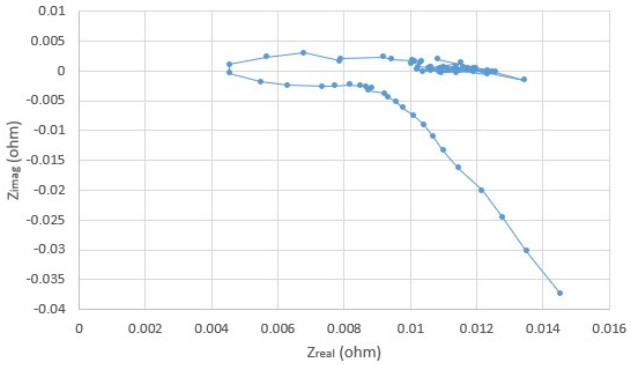

(a) Nyquist plot

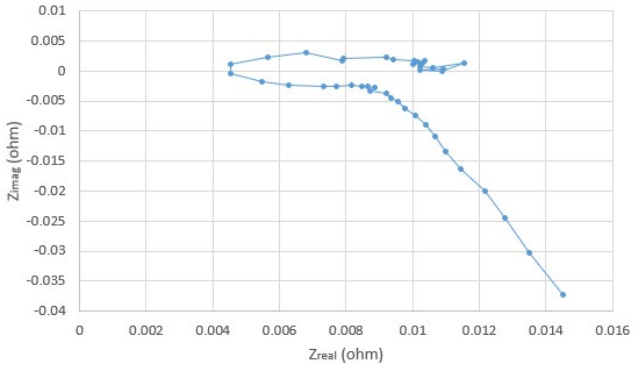

(b) Nyquist plot without low frequencies

Figure 7.7. Nyquist plot (a) and Nyquist plot without low frequencies (b)

The loop in the middle of the figure represents the chemical reaction resistance. The form of the arc and the very low resistance obtained indicate the presence of a short circuit. The chemical reaction is not correctly represented due to the short circuit.
The big instability in the middle of the figures is caused by the short circuit and the noise the bubbles cause. The negative straight line represents inductive noise, which is not valuable for the purpose of the test.[35] [36] [37] [38]

A Bode plot with low frequencies filtered can be observed in figure 7.8. It also shows considerable inductive noise, due to the quick increase after 10000 Hz.

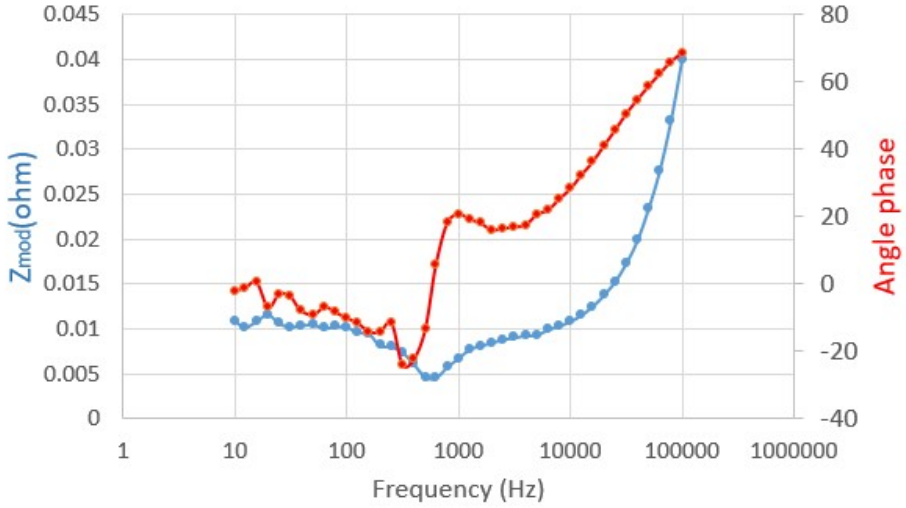

Figure 7.8. Bode plot

7.2.4 Test 4

An increase in performance is expected in the first 3 weeks of operation, reaching the performance peak at some point between the first 250 to 500 hours, when the catalyst active sites and transport pathways are maximized. Then, degradation effects will play a more important role and performance would decrease over time.[45]

This peak was found to be at 264 hours after the beginning of the experiment, the voltage obtained was 1.84V. Table 7.2 shows the different voltages obtained at different times of operation:

Table 7.2. Voltage evolution over time

Time (h)	Voltage (V)	Temperature (°C)
264	1,84	78,0
310	1,87	78,0
360	1,87	76,0
430	1,88	77,8

In this case, other factors must be taken into account when reaching a conclusion. Temperature instability was present during the experiment, the measurements made at 264 hours were taken at 78°C and the ones made at 360 hours were taken at 76°C. Higher temperatures decrease the voltage needed, so, if they were at the same temperature the would be less voltage difference. It was conclude that the peak performance point was reached at 264 hours.

It was observed how the cathode output flow drops periodically, as can be seen in figure 7.9. This could mean that oxygen is being accumulated inside the electrolyzer, a safety measurement is activated, lowering the inlet flow until the problem is solved

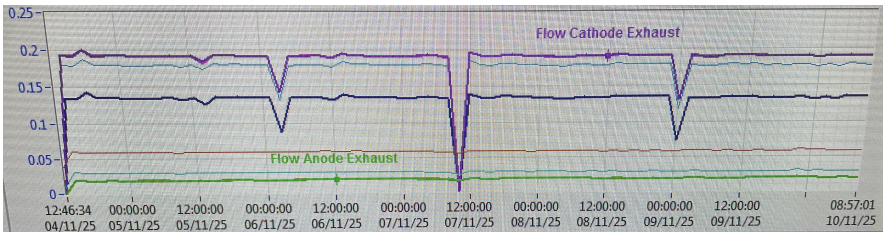

Figure 7.9. Cathode flow instability

An increase in pressure was also observed in the display of the station, it increased from 2.4 to 3.4 barg. It could indicate the malfunctioning of the station or electrolyzer, it could be a water accumulation inside the electrolyzer.

7.2.5 Test 5

After the continuity of the malfunctioning of the cell and to try to fix the overvoltage problem, it was disassembled again, and the cathode side gasket and GDL were replaced on 14th November. It was believed that the 3 GDLs were causing internal resistance, so they were substituted for a singular GDL, with a thickness of 0.28 mm, the gasket of 0.5 mm was substituted for a thinner one, of 0.25 mm, to not overlap the GDL.

Later, the electrolyzer was checked and normal operation was resumed. Same conditions as before were applied. The IV curve extracted from the test, at 76.5°C, is shown in figure 7.10:

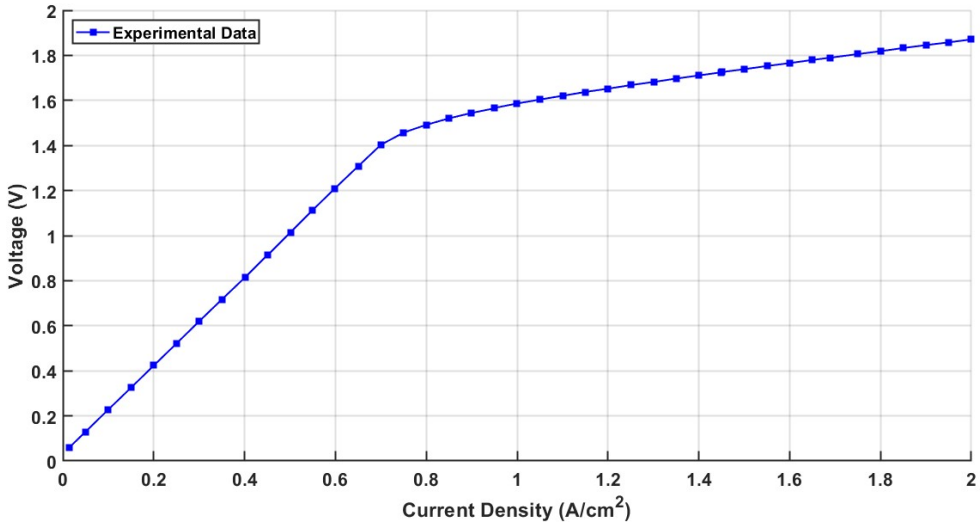

Figure 7.10. I-V curve at 76.5°C (14/11/2025)

This change had no noticeable effect on the electrolyzer behavior.

The 19th of November, a leak was discovered when increasing the water recirculation flow and electrolyzer pressure. It was probably caused by the change in the components thickness, the lack of heat pretreatment of gaskets, due to wrong assembly, or due to a compression loss. A disassembly was performed to fix the leak and identify possible soft shorts.

The electrolyzer was left disassembled to let the components dry and to facilitate the problem identification. The GDL area was reduced to try to avoid possible overlap with the gasket, which could be a possible explanation of the overvoltage error. As a result of this actions, the electrolyzer could not operate as intended, and data could not be used for the conditions of this experiment, moving on to the ”second experiment”

7.2.6 IV comparison

Figure 7.11 shows the IV curve of the first and last measurement of this experiment setup. There is a difference of approximately 312 hours between the measurements.

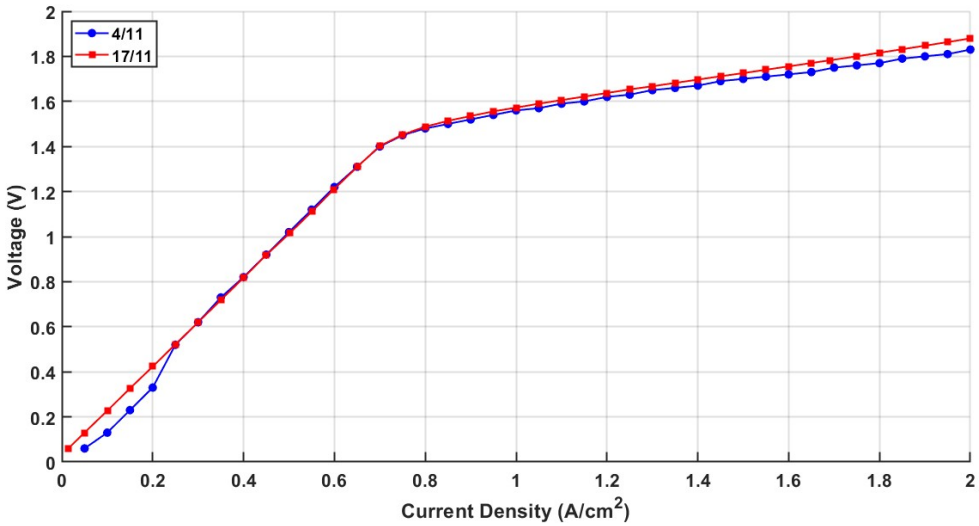

Figure 7.11. IV curve comparison

The 4/11 was measured at 78°C and the 17/11 at 77.8°C. It can be observed that the voltage for the latest experiment is higher. This corresponds to the expected behavior, since the degradation causes more internal resistance, increasing the ohmic losses.
Even with the overvoltage problem at low current densities, some degradation can be noticed.

7.3 Second experiment

This part corresponds to the electrolyzer operation after changing the 3 GDL for only one of the new 0.28 mm thickness GDL. Figure 7.12 shows the IV curve of the electrolyzer. It can be observed that the voltage reached is higher than the one obtained in the first experiment, it increases from 1.83V to 2.07V. This means that the efficiency is lower than the one obtained before.

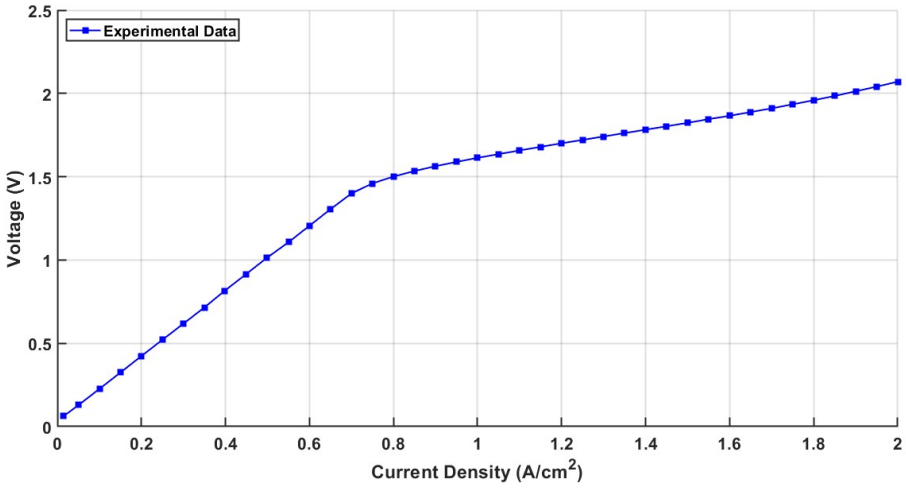

Figure 7.12. I-V curve at 77°C (21-11-2025)

Possible causes that could explain this difference are mainly mechanical causes:

- The membrane was dried, and then DI water was used to wet it again to make the assembly easier. This could cause some damage to the membrane functioning.

- Three GDLs with a total thickness of 0.57mm were changed for one layer of 0.28mm, this originates a compression loss in the electrolyzer. The contact between the components inside the cell is not as strong and efficient as before, so contact resistance increases, and more voltage is needed to surpass this resistance.

- The PTL has the footprint of the flow plates pattern on one side, as can be seen in figure 7.13. When the electrolyzer was assembled, the PTL was flipped, leaving the flow pattern face the membrane. The flow pattern footprint can lead to an uneven surface, which reduces the contact efficiency and increases the resistance.

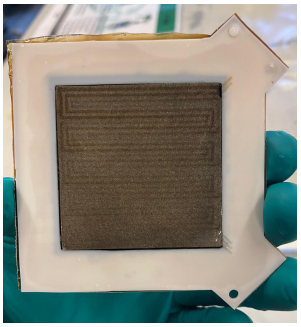

Figure 7.13. PTL with flow pattern footprint

The electrolyzer ran for more than 48 hours, obtaining a very unstable operation. The water recirculation flow could not be kept constant and the hydrogen produced varied drastically, as can be seen in figure 7.14:

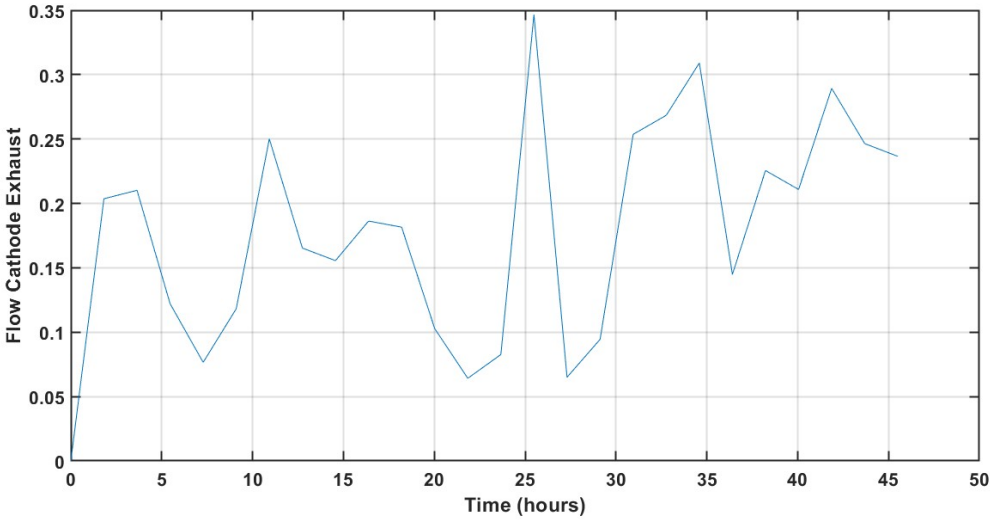

Figure 7.14. Cathode flow output

After noticing this, it was decided to not continue with the experiment. The electrolyzer ran for 528 hours. However, final measurements were taken to check the electrolyzer at different condition. IV curves from 0 to 3 A/cm^2 and from 0 to 6 A/cm^2 were performed, as can be seen in figure 7.15 and figure 7.16, respectively.

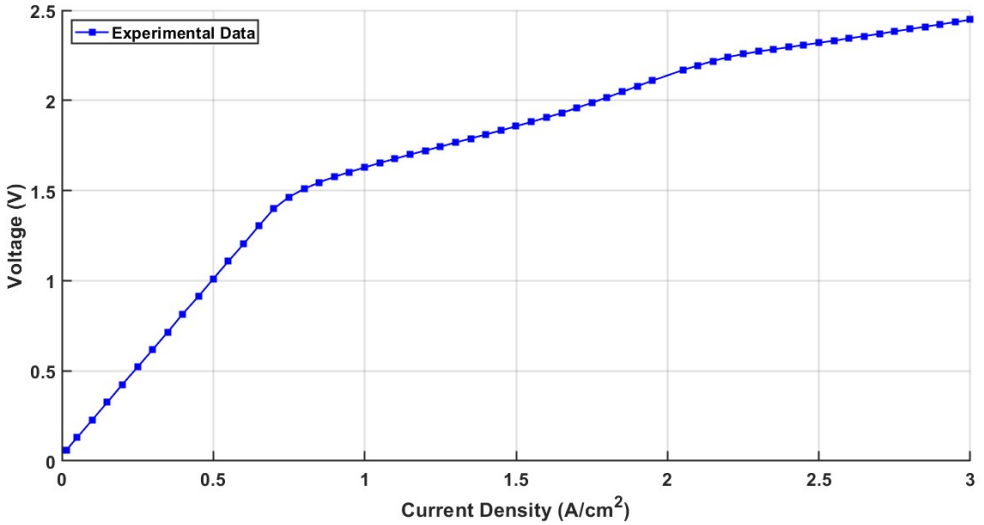

Figure 7.15. I-V curve up to 3 A/cm^2

The behavior of these IV curves is not as expected. It was expected to see a exponential increase after some point at high current density. However, it can be observed how the voltage increases linearly from 0.75 A/cm^2 to 2.3 A/cm^2, and then it increases linearly again but with a slightly different slope.
This is believed to be caused by the short circuit and the wrong electrolyzer functioning. The self-heating effect is probably dominant at high current densities for this set up, enhancing the reaction kinetics and countering the effect of mass transport losses, which are the causes

of the exponential voltage increase at high current densities. This gives a linear increase as a result. [46]

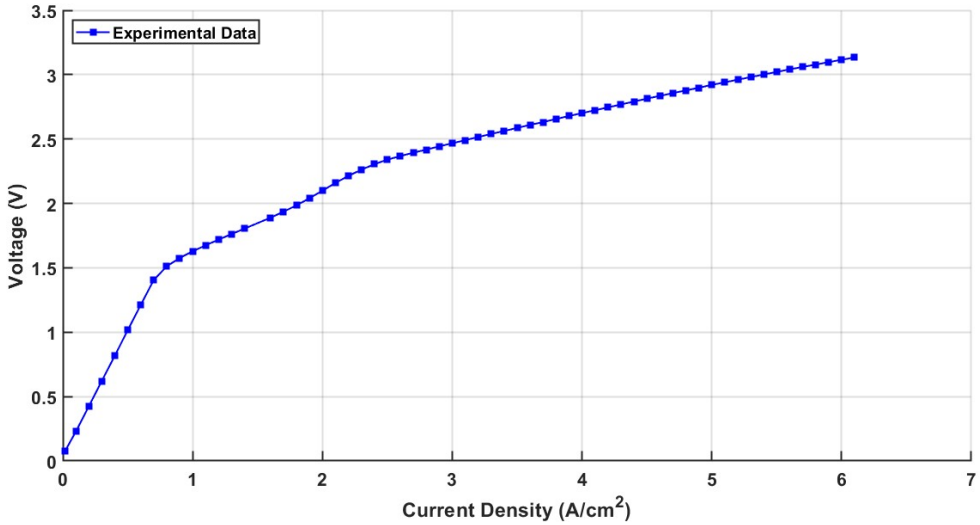

Figure 7.16. IV curve up to 6 A/cm^2

Figure 7.17 shows the IV curve for three different temperatures. The result is as expected, at higher temperatures, less voltage is needed. There is a bigger difference between the 50°C and 68°C than from 68°C to 77°C, which makes sense since the kinetics follow an exponential behavior respect to temperature, following Arrhenius law.

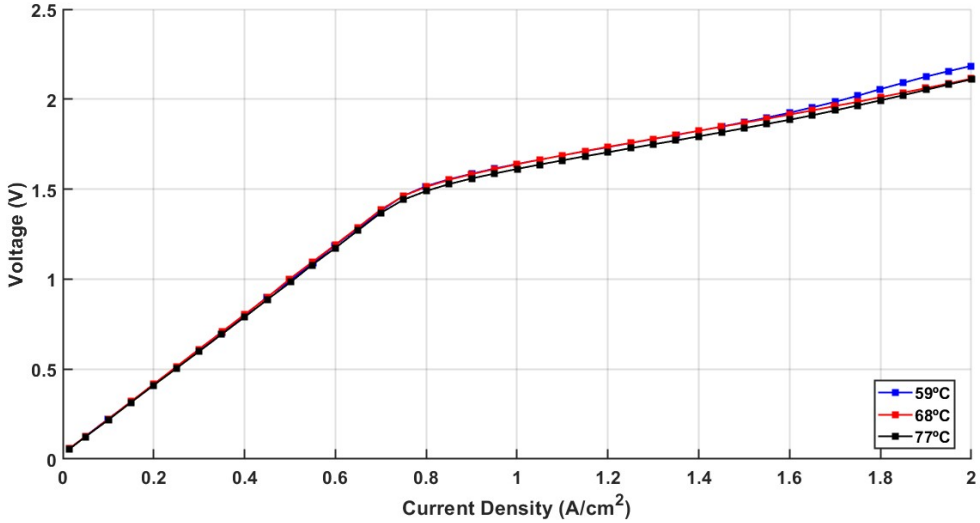

Figure 7.17. Temperature IV curve comparison

It was also observed that tightening the cell and compressing it increases the efficiency for this scenario. The voltage drops from 2.11 to 2.06V. The contact efficiency between layers and the efficiency increase as a consequence of compression.

7.4 Degradation experiment

This acceleration degradation test was performed with the goal of observing significant degradation of any electrolyzer components.
The electrolyzer was operated under the same conditions as in previous experiments, but with one big difference between them. The GDL made of carbon paper is used both as GDL and PTL, using two GDLs in the anode, and one in the cathode. The thickness of each GDL is 0.28mm and the gasket thickness is 0.50 mm.

Literature states that the electrolyzer can work properly in the first 40 hours when using carbon based materials as PTL. Figure 7.18 shows the evolution of the voltage over time, it can be seen how degradation starts to have a remarkable effect after 110 hours of operation. It increases rapidly after 120 hours, indicating severe damage, loss of contact and a catastrophic failure. [47]
The electrolyzer is supposed to work under constant conditions. However, the same phenomena of periodically electrolyzer deactivation is observed here, at 45 and 68 hours of operation. Cell conditioning was not performed in this electrolyzer, which could explain the instability in the first 20 hours. [47]

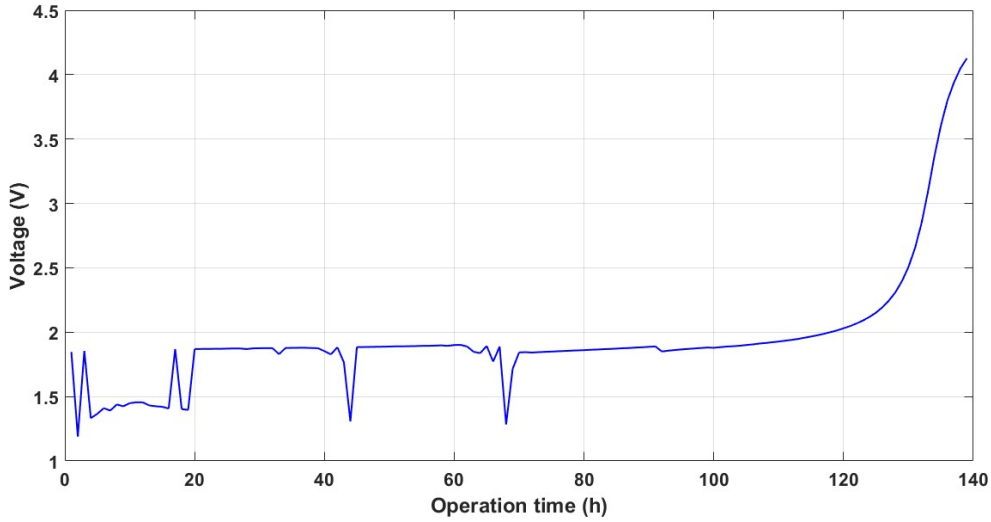

Figure 7.18. Voltage over time

Degradation occurs mainly as a result of carbon corrosion on the PTL side. Longer periods of operation than 40 hours can cause the destruction of the anode flow field. [47]

Figure 7.19 shows the anode GDL that was in contact with the membrane. It is wet and bent, the thickness was measured and found to be reduced from 0.31 to 0.21 mm. This measurement can be not very precise because of the humidity of the layer and the method used to measure it, but it definitely shows considerable thickness reduction, which would agree with the carbon corrosion of the GDL. The thinning proves the strong carbon oxidation of carbon based materials for the OER. Is worth to mention that the second carbon paper layer, the one not facing the membrane, was untouched.

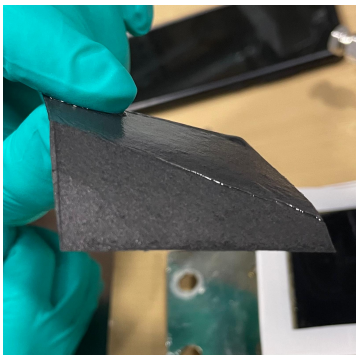

Figure 7.19. PTL bent

7.5 Degradation overview

Different kinds of degradation could be observed during the experiment, two types of degradation were clearly identified:

- Reversible degradation: it was always present in the experiment, the voltage increased by a small amount after some time of operation. It is mainly due to bubbles, which are formed during the operation, and act as a resistance inside the electrolyzer. When the electrolyzer was turned off or during the IV curve measurement, these reversible degradation was vanished.

- Carbon corrosion: it was observed when using the carbon paper as the PTL. The thickness and the mechanical stability of the layer was significantly reduced due to the carbon oxidation.

Other kinds of degradation also took place, but they could not be easily identified. However, a list of the most probable degradation mechanisms which took place is provided:

- Chemical ionomer degradation: the radicals attack to the membrane is one of the most dominant degradation mechanisms when the electrolyzers are operated at 80°C. It induces the membrane thinning. [16]

- PTL passivation: the Ti from the PTL reacts with water to form an oxide layer, which decreases the efficiency of the PTL. This kind of degradation is reduced by using the coating materials, but high temperatures enhance this mechanism to happen.

- Catalyst dissolution: Iridium oxide is dissolved in acidic environment and at high potentials, decreasing the catalyst surface area and its efficiency. This mechanism is accelerated at 80°C.

7.6 Electrolyzer malfunctioning

On 9 December, a short circuit was found to be the reason for the electrolyzer malfunctioning, electricity follows a direct path through the electrolyzer instead of following the intended route and it creates a parallel pathway for the electrons. This can be confirmed by observing how the voltage increases linearly from 0, following Ohm's Law instead of Tafel equation. It was caused by the connection between the pipes and the electrolyzer.
Small plastic tubes were added between the pipes and the electrolyzer connections as a non electrical conductive bridge between them. Figure 7.20 shows the electrolyzer with the mentioned plastic tubes:

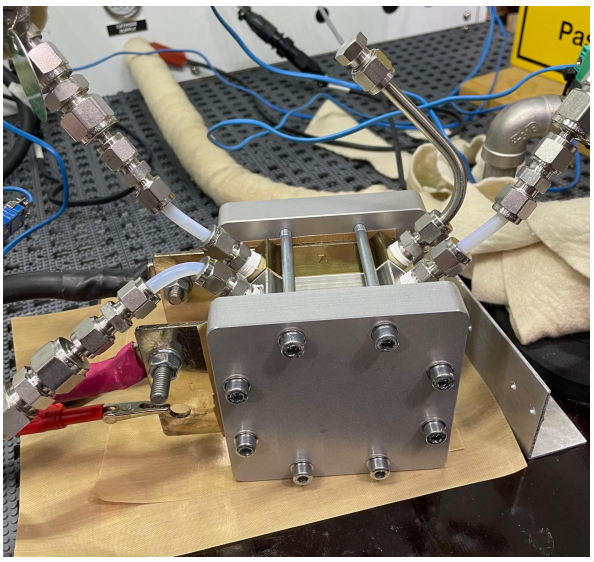

Figure 7.20. Electrolyzer with plastic tubes

Additionally, the possible reasons for electrolyzer malfunction discussed before finding the cause of the short circuit are reviewed in this section.
The electrical resistances of all the components and the electrolyzer as a cell were checked and confirmed to be in an acceptable range. Different options were found to be the possible reason for the short circuit:

1. Gaskets malfunction: incorrect gasket positioning or wrong gasket thickness selection can cause a short circuit. Metal plates can get in contact, creating a path for the electrons to go through.

2. Mechanical failure: too much compression can also deform the gaskets and create a short circuit. Other more unlikely possibility is the carbon paper material of the GDL crossing the membrane and directly touching the PTL with punching fibers, creating a direct path for the electrons. This can happen when too much torque pressure is applied. [48]

3. Materials and components used: they should not represent a problem for the electrolyzer proper functioning, but maybe some anomaly with the bought components could cause the electrical short circuit.

Nyquist plot from figure 7.7b shows very low resistances, it indicates that there is a electrical short circuit with very low resistance, which allows the electricity to pass through.
The short circuit would also explain why an exponential increase at high current densities is not observed, since the voltage follows Ohm's Law.

Other possibility was just the malfunctioning of the test station. Two electrolyzers with different inner components were tested, obtaining the same problem, so the problem could be inside the test station.

7.7 Electrolyzer with no electrical short circuit

7.7.1 IV curve

The data obtained after the electrical short circuit was fixed are presented in this section. Figure 7.21 shows the IV curve of the electrolyzer at 71.5° C. It can be observed how it behaves as expected, with an exponential increase in the beginning due to the activation overpotential, and then a linear increase due to the ohmic overpotential.

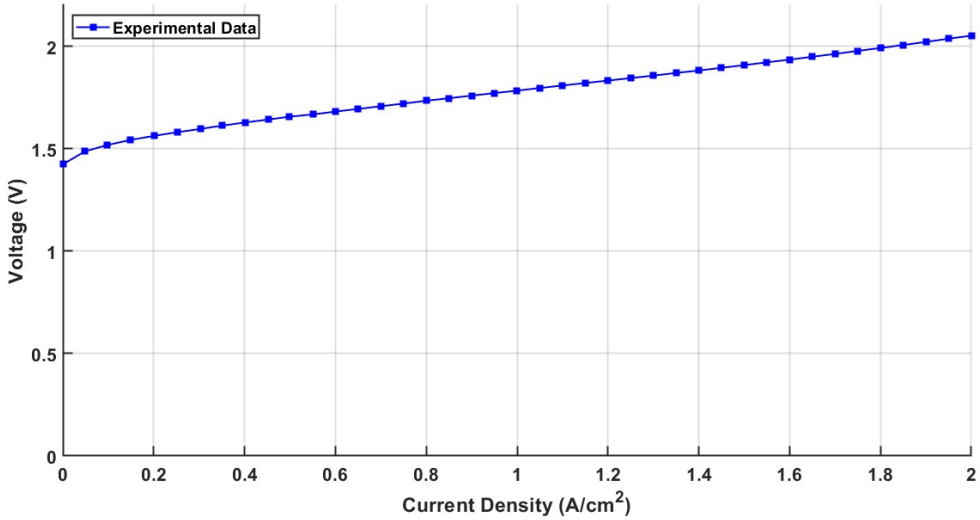

Figure 7.21. IV curve at 71°C with no short circuit (10-12-2025)

The electrolyzer used for this test was the same used for the accelerated degradation test. It presents some degradation or inefficiency. That could explain why the initial point is a bit higher than the expected one, the reversible potential. The IV curve was also measured immediately after normal operation, so the electrolyzer could still be electrically charged.

The problem of low oxygen measurement still persists. However, hydrogen production increased from around 0.19 to 0.35 NLPM. This shows a considerable increase in efficiency. The Faradaic efficiency of this electrolyzer will be compared to the previous one in the next section.

7.7.2 EIS

An EIS test was also performed at 71.5 ° C and 2 A/cm^2 for this electrolyzer. Figure 7.22 shows the Nyquist plot obtained, frequencies lower than 10 Hz and higher than 10000 Hz were not taken into account because of the reasons explained above. The main difference between this plot and the one with the short circuit is the arc or curvature that can be seen in the graph. It represents the charge transfer resistance of the electrochemical reaction.

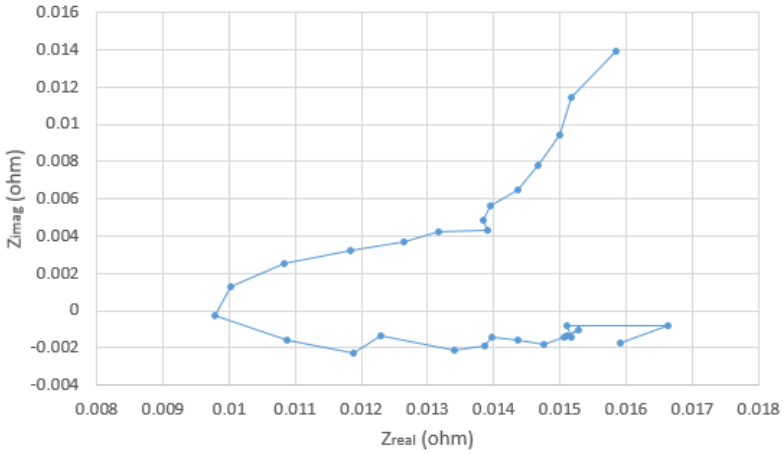

Figure 7.22. Nyquist plot

Figure 7.23 shows the Bode plot of this electrolyzer. This graph shows a higher resistance that the one obtained for the short circuit, indicating that the short circuit is non existent anymore.

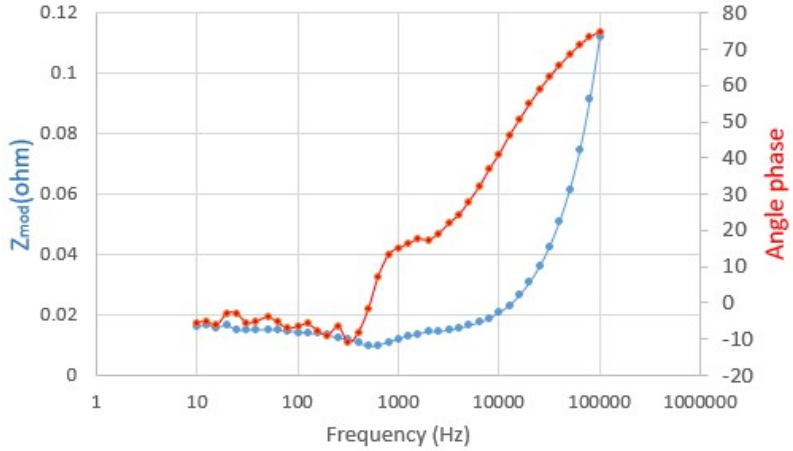

Figure 7.23. Bode plot

7.8 Model

A model was developed to process the results and obtain a clearer vision of the electrolyzer performance and resistances. The code is presented in Appendix section.
The data taken as a reference are the data-points obtained on November 10th.

7.8.1 Exchange current density

The exchange current density is represented in figure 7.24. It was calculated by using the Faraday's Law, and the hydrogen produced and overpotential experimental data. The data considered were only those obtained after the reaction occurred.

The Y axis represents the overpotential (η) applied to the electrolyzer, following equation (7.1):

$$\eta = V_{exp} - V^{\circ} \tag{7.1}$$

Where V_{exp} is the experimental voltage measured and V° is the reversible potential.

The X axis is the electrical current calculated from the Faraday equation (I_{ec}), using the experimental hydrogen produced data. It is expressed on a logarithmic scale to linearize the Tafel equation:

$$\eta = b \cdot log(I_{ec}) + a \tag{7.2}$$

By doing this, the slope (b) is obtained. This term is the Tafel slope, which represents the sensitivity of the current to the applied overpotential, and gives an idea of the electrochemical reaction rate. The intercept (a) of the Tafel fit is also obtained.

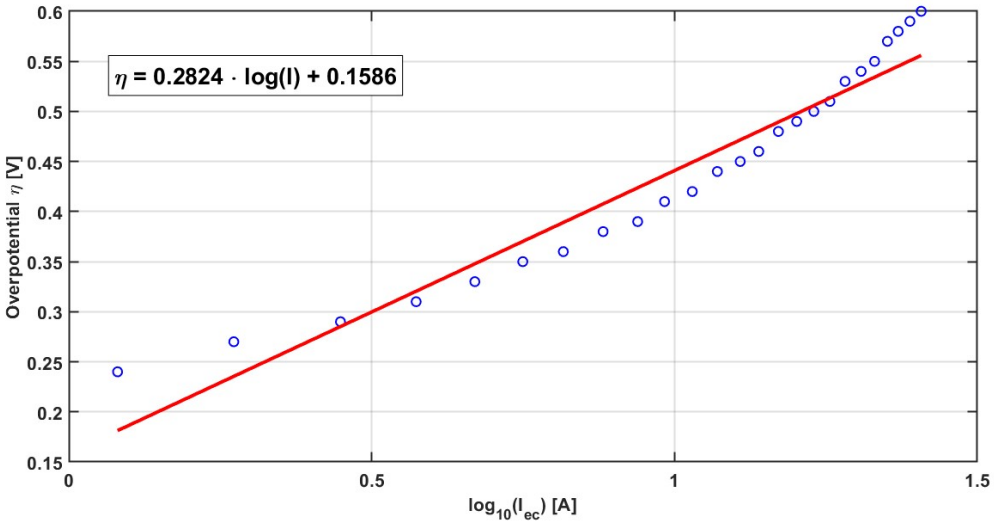

Figure 7.24. Tafel fit

The Tafel fit equation obtained is presented in equation (7.3):

$$\eta = 0.2824 \cdot log(I) + 0.1586 \tag{7.3}$$

After calculating I for $\eta = 0$ and dividing by the area of operation, the exchange current density calculated was found to be $1.1{\cdot}10^{-2}$ A/cm^2.
A high exchange current density value usually means higher catalyst activity and better

performance. The value obtained is significantly higher than the ones found in the literature. [49]
However, it is believed to be a consequence of the electrolyzer malfunction and the electrical short circuit. It was not possible to verify it with the data obtained for the electrolyzer with no short circuit due to a problem with the hydrogen production measurement device. Only the hydrogen produced at 2A/cm^2 could be recorded. the same applies to the Faradaic efficiency.

7.8.2 Resistances

The IV curve obtained with experimental data is represented in figure 7.25. A distinction between two sections is made:

- First zone: it represents the initial zone, in which the reaction does not take place due to the electrical short circuit. The voltage here increases linearly, and the resistance is 0.078 $\Omega \cdot cm^2$.

- Second zone: it starts when the reaction begins to occur. The voltage increases more slowly than for the first section. It increases linearly, following the ohmic losses, and the resistance is also lower, with a value of 0.012 $\Omega \cdot cm^2$.

The lower value of the resistance in the second zone indicates that electrons find an easier path through the reaction than through the resistance presented by the electrical short circuit. A parallel circuit inside the electrolyzer is created by the reaction. The resistance is also calculated for the experimental data for the electrolyzer with no short circuit, obtaining a value of 0.274 $\Omega \cdot cm^2$.

A theoretical IV curve is also plotted, it is calculated by using standard values of membrane resistance and exchange current densities of anode and cathode. [49] [50]. A comparison between the three IV curves can be seen in figure 7.25:

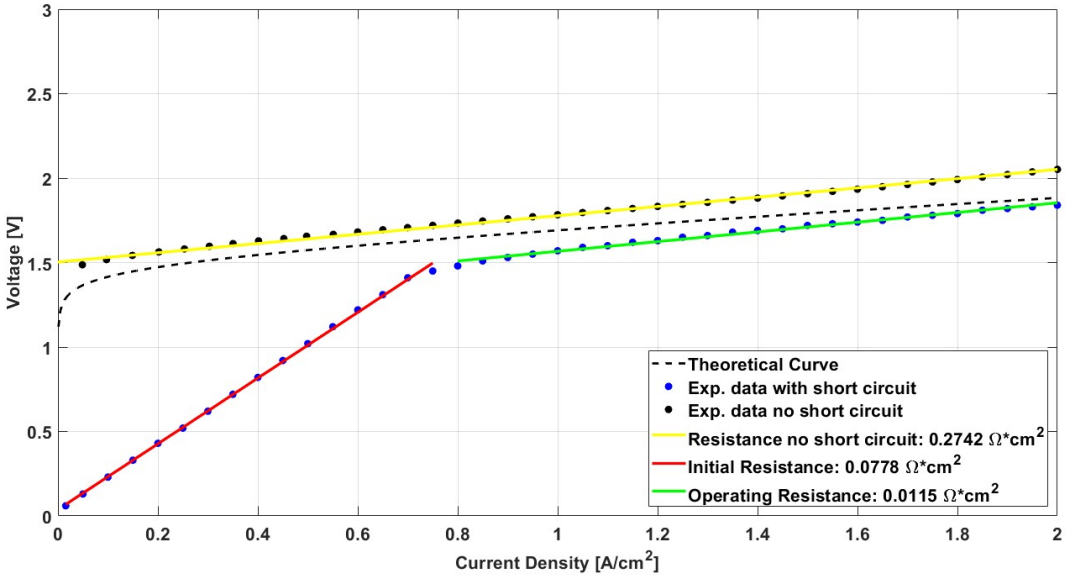

Figure 7.25. Theoretical and experimental IV curve with slope fit

It can be observed how different the IV curves are before starting the reaction for both cases. The reaction must start at very low current densities and reach the thermoneutral potential rapidly, as the theoretical curve shows. However, there is a less resistant path for the electrons to go through the short circuit and the reaction does not happen.
When the thermoneutral potential is reached in the experiment, the reaction starts to occur.

7.8.3 Faradaic efficiency

A Faradaic efficiency plot is presented in figure 7.26. It shows how hydrogen is not produced until the thermoneutral potential is reached, at 0.75 A/cm^2. Then, hydrogen starts to be produced and the faradaic efficiency increases. It does not increase linearly because of the nature of the reaction kinetics and Tafel behavior, Described in equation (7.2)

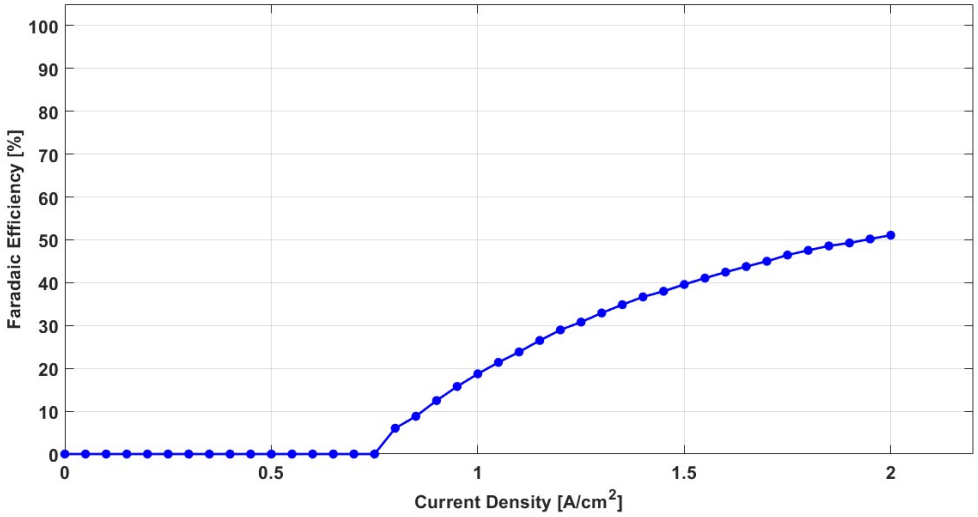

Figure 7.26. Faradaic efficiency

The Faradaic efficiency of the electrolyzer with no short circuit is not plotted because there was a problem with the hydrogen production measurement device. The Faradaic efficiency was around 99% at this point, as it was expected.

Conclusion 8

This project was carried out with the main purpose of studying the electrolyzer operation and its degradation over time.
To achieve this goal, an electrolyzer was experimentally tested in the Greenlight Innovation electrolyzer test equipment. The electrolyzer was assembled manually in the lab.

An electrical short circuit was present throughout all the experiments, causing the electrolyzer to deviate from expected behavior at low current densities, and lowering its performance. This problem persisted and caused unplanned actions in the electrolyzer set up. The data obtained and the experiment procedure followed were strongly influenced by the electrical short circuit. It was caused by the metallic connection between the pipes and the electrolyzer. The short circuit was identified and fixed too late to obtain high-quality degradation data, so only the IV curve obtained and the EIS test are discussed.

Irreversible degradation was observed during the experiment, showing that the electrolyzer efficiency decreases over time after reaching the performance peak at 264 hours of operation. The mechanisms attributed to the irreversible degradation are chemical ionomer degradation, PTL passivation, catalyst dissolution and carbon corrosion.

Another test was performed to test the degradation induced by carbon corrosion, expected results were obtained. Significant thinning was observed in the carbon paper layer used as PTL, demonstrating the strong carbon consumption and incompatibility of carbon-based materials for the OER.

Reversible degradation was present throughout all the experiments. It was observed multiple times how the voltage increased after some time at constant operation parameters. When the experiment was stopped, it was also noticed how the degradation was reversed. The voltage reached after turning on the electrolyzer again was lower than the voltage before it was turned off. This kind of degradation is mostly caused by oxygen bubbles stuck inside the electrolyzer.

An EIS test was also performed to obtain more information about the internal resistances of the electrolyzer. However, the data obtained were not very useful for this purpose. Instead, it was helpful to understand how to interpret an EIS test, and to support the hypothesis of having an electrical short circuit inside the electrolyzer.

It was proven that electrolyzer performance improves at higher temperatures, and it is not affected by the water recirculation flow and pressure.

Future Work 9

9.1 Experimental set-up

Due to all the issues presented with this experimental set-up, it would be helpful to test the electrolyzer in a different laboratory set-up. This would allow to obtain information about the cause of the problems.

9.2 Longer and continuous experiment

Due to problems with the set-up, the experiment could not reach the aim of 1000 hours of operation. The operation was also stopped multiple times to disassemble the electrolyzer and try to fix the problems.
It would be very interesting to have data points up to or for more than 1000 hours of continuous operation. Degradation would be more noticeable and easier to identify.

9.3 Operation conditions

The experiment was performed at a fixed temperature and pressure. Operation conditions play a key role in the degradation effects. Other conditions could be studied and linked to different degradation mechanisms.

9.4 Model development

A simulation model can be developed based on the experimental data obtained. It could simulate the electrolyzer performance and predict the lifetime, taking into account the degradation effects.

Bibliography

[1] Shengjie Peng. *Electrochemical Hydrogen Production from Water Splitting: Basic, Materials and Progress*. Book. Springer Nature Singapore Pte Ltd, 2023. ISBN: 978-981-99-4467-5. DOI: 10.1007/978-981-99-4468-2.

[2] Eva Wallnöfer-Ogris et al. "A review on understanding and identifying degradation mechanisms in PEM water electrolysis cells: Insights for stack application, development, and research". In: *International Journal of Hydrogen Energy* 65.35 (2024), pp. 381–397. DOI: 10.1016/j.ijhydene.2024.04.017.

[3] U.S. Department of Energy. *Technical Targets for Proton Exchange Membrane Electrolysis*. 2022. URL: https://www.energy.gov/eere/fuelcells/technical-targets-proton-exchange-membrane-electrolysis.

[4] Dmitri Bessarabov et al., eds. *PEM Electrolysis for Hydrogen Production: Principles and Applications*. CRC Press, 2016. ISBN: 9781498769148. DOI: https://doi.org/10.1201/b19096.

[5] M. S. Thomassen et al. "PEM water electrolysis". In: *Electrochemical Power Sources: Fundamentals, Systems, and Applications*. Ed. by T. Smolinka and J. Garche. Chapter in edited book. Elsevier, 2022, pp. 199–228. ISBN: 978-0-12-819424-9. DOI: 10.1016/B978-0-12-819424-9.00013-6.

[6] Cliffton Ray Wang et al. "Proton Exchange Membrane (PEM) Water Electrolysis: Cell-Level Considerations for Gigawatt-Scale Deployment". In: *Chemical Reviews* 125.2 (2025), pp. 1257–1298. DOI: 10.1021/acs.chemrev.3c00904.

[7] Marco Antonio Di Francia et al. "Electrospun catalysts for PEMFC and PEMWE: A path to sustainable and efficient energy conversion". In: *International Journal of Hydrogen Energy* 138.16 (2025), pp. 352–367. DOI: 10.1016/j.ijhydene.2025.352367.

[8] Yulan Peng et al. "Non-precious transition metal-based OER catalysts for PEM water electrolysis: a mini review". In: *Research on Chemical Intermediates* 51.8 (2025).

[9] S. Stucki et al. "PEM water electrolysers: evidence for membrane failure in 100 kW demonstration plants". In: *Journal of Applied Electrochemistry* 28.10 (1998), pp. 1041–1049. DOI: 10.1023/A:1003477305336.

[10] Shan Luan and Jiujun Zhang. "Membrane degradation mechanisms in PEM fuel cells". In: *Catalysis Today* 202.1 (2012), pp. 103–113. DOI: 10.1016/j.cattod.2012.09.031.

[11] M. Chandesris et al. "Membrane degradation in PEM water electrolyzer: Numerical modeling and experimental evidence of the influence of temperature and current density". In: *International Journal of Hydrogen Energy* 40.3 (2015), pp. 1353–1366. DOI: 10.1016/j.ijhydene.2014.11.111.

[12] Ashkan Makhsoos et al. "Proton exchange membrane water electrolyzers degradation models review: implications for power allocation and energy management". In: *Journal of Power Sources* 655 (2025), p. 238003. DOI: 10.1016/j.jpowsour.2025.238003.

[13] Bonanno et al. “Review and Prospects of PEM Water Electrolysis at Elevated Temperature Operation”. In: *Advanced Materials Technologies* 9.2 (2024), p. 2300281. DOI: 10.1002/admt.202300281.

[14] Eveline Kuhnert et al. “Analysis of PEM Water Electrolyzer Failure Due to Induced Hydrogen Crossover in Catalyst-Coated PFSA Membranes”. In: *Membranes* 13.3 (2023), p. 348. DOI: 10.3390/membranes13030348.

[15] Annik Bernhardt et al. “Degradation Mechanisms in PEM Electrolyzers – Occurrence, Relevance and How We Can Measure Them”. In: *EFCF 2025: Low-Temperature Fuel Cells, Electrolysers H Processing*. Lucerne, Switzerland, 2025, B1004. URL: https://www.efcf.com/fileadmin/user_upload/EFCF-2025_Paper_B1004_10909_PEFC_PEMWE-Degradation_Bernhardt_Annik.pdf.

[16] Kryštof Foniok et al. “Mechanisms and Modelling of Effects on the Degradation Processes of a Proton Exchange Membrane (PEM) Fuel Cell: A Comprehensive Review”. In: *Energies* 18.8 (2025), p. 2117. DOI: 10.3390/en18082117.

[17] Eva Wallnöfer-Ogris et al. “Main degradation mechanisms of polymer electrolyte membrane fuel cell stacks – Mechanisms, influencing factors, consequences, and mitigation strategies”. In: *International Journal of Hydrogen Energy* 50.B (2024), pp. 1159–1182. DOI: 10.1016/j.ijhydene.2023.06.215.

[18] Yuhao Chen et al. “Key Components and Design Strategy for a Proton Exchange Membrane Water Electrolyzer”. In: *Small Structures* 4.6 (2022), p. 2200130. DOI: 10.1002/sstr.202200130.

[19] Mingzhang Pan et al. “A review of membranes in proton exchange membrane fuel cells: Transport phenomena, performance and durability”. In: *Renewable and Sustainable Energy Reviews* 141 (2021), p. 110771. DOI: 10.1016/j.rser.2021.110771.

[20] Hee-Sun Shin and Byeong Soo Oh. “Water transport according to temperature and current in PEM water electrolyzer”. In: *International Journal of Hydrogen Energy* 46.29 (2021), pp. 17627–17636. DOI: https://doi.org/10.1016/j.ijhydene.2019.10.209.

[21] Ahmadreza Rahbari et al. “Electro-osmotic Drag and Thermodynamic Properties of Water in Hydrated Nafion Membranes from Molecular Dynamics”. In: *The Journal of Physical Chemistry C* 126.18 (2022), pp. 8121–8133. DOI: 10.1021/acs.jpcc.2c01226.

[22] M. Bernt et al. “Analysis of Gas Permeation Phenomena in a PEM Water Electrolyzer Operated at High Pressure and High Current Density”. In: *Journal of The Electrochemical Society* 167.12 (2020), p. 124502. DOI: 10.1149/1945-7111/abaa68.

[23] Khaja Wahab Ahmed et al. “Effect of Components and Operating Conditions on the Performance of PEM Electrolyzers: A Review”. In: *Electrochem* 3.4 (2022), pp. 581–612. DOI: 10.3390/electrochem3040040.

[24] Maximilian Schalenbach et al. “Gas Permeation through Nafion. Part 1: Measurements”. In: *The Journal of Physical Chemistry C* 119.45 (2015), pp. 25145–25155. DOI: https://doi.org/10.1021/acs.jpcc.5b04155.

[25] Vincenzo Liso. *Fuel cell system fundamentals, Lecture 2*. Presented in a lecture of the curse named Fuel Conversion and Production (TEPE2,HYTEC2,FPS2) [C-AE-M] - F25 at Aalborg University. 2025. URL: https://www.moodle.aau.dk/pluginfile.php/3641148/mod_resource/content/0/2.VLI%202024%20Fuel%20conversion%20and%20production-2025.pdf.

[26] Sarah J. Blair et al. "Reversible Losses in Proton Exchange Membrane Water Electrolysis". In: *Journal of The Electrochemical Society* 172 (2025), p. 034517.

[27] Steffen Henrik Frensch et al. "Model-Supported Analysis of Degradation Phenomena of a PEM Water Electrolysis Cell under Dynamic Operation". In: *ECS Transactions* 85.11 (2018), p. 37. DOI: 10.1149/08511.0037ecst.

[28] *Greenlight Innovation: Fuel Cell and Electrolyzer Test Equipment*. https://www.greenlightinnovation.com/. Accessed: 2025-10-XX. 2025.

[29] Bekaert. *Titanium for PEM Hydrogen Electrolysis Technology*. https://www.bekaert.com/en/hydrogen-generation/hydrogen-electrolysis-technology/pem/titanium. Accessed: 20 ::contentReference[oaicite:0]index=0. 2025.

[30] Fuel Cell Store. *Toray Carbon Paper 060*. https://www.fuelcellstore.com/fuel-cell-components/gas-diffusion-layers/carbon-paper/toray-carbon-paper/toray-carbon-paper-060-pack. Accessed: 2025-11-10. 2025.

[31] G. Bender et al. "Initial approaches in benchmarking and round robin testing for proton exchange membrane water electrolyzers". In: *International Journal of Hydrogen Energy* Journal 44 (2019), pp. 9174–9187. DOI: https://doi.org/10.1016/j.ijhydene.2019.02.074.

[32] Weitian Wang et al. "Exploring the Impacts of Conditioning on Proton Exchange Membrane Electrolyzers by In Situ Visualization and Electrochemistry Characterization". In: *ACS Applied Materials Interfaces* 14 (7) (2022), pp. 9002–9012. DOI: https://doi.org/10.1021/acsami.1c21849.

[33] Shaun Alia Elliot Padgett Guido Bender. *Membrane Pretreatment and Cell Conditioning for Proton Exchange Membrane Water Electrolysis*. Tech. rep. 2021. DOI: https://docs.nrel.gov/docs/fy23osti/80955.pdf.

[34] Gamry Instruments. *Reference 3000 Potentiostat/Galvanostat/ZRA — High-Performance Instrument for Electrochemical Energy and Research*. https://www.gamry.com/potentiostats/reference/reference-3000/. Accessed: 2025-11-10. 2025.

[35] Gantner Instruments. *Electrochemical Impedance Spectroscopy (EIS) – Easy-to-Integrate Multi-Channel High-Power Solution*. https://www.gantner-instruments.com/products/special-products/electrochemical-impedance-spectroscopy/. Accessed: 2025-11-06. 2024.

[36] Hend S. Magar, Rabeay Y. A. Hassan, and Ashok Mulchandani. "Electrochemical Impedance Spectroscopy (EIS): Principles, Construction, and Biosensing Applications". In: *Sensors (Basel)* 21.19 (2021). Ed. by Huangxian Ju, p. 6578. DOI: 10.3390/s21196578.

[37] Xinyi Huo et al. "Impedance analysis of alkaline water electrolysis based on distribution of relaxation time". In: *International Journal of Hydrogen Energy* 53 (2024), pp. 684–697. DOI: 10.1016/j.ijhydene.2023.12.086.

[38] Jun Huang et al. “Graphical analysis of electrochemical impedance spectroscopy data in Bode and Nyquist representations”. In: *Journal of Power Sources* 309 (2016), pp. 82–98. DOI: 10.1016/j.jpowsour.2016.01.073.

[39] Muthumeenal Arunachalam and Dong Suk Han. “Efficient solar-powered PEM electrolysis for sustainable hydrogen production: an integrated approach”. In: *Emergent Materials* 7.4 (2024). DOI: 10.1007/s42247-024-00697-y.

[40] PalmSens BV. *Bode and Nyquist Plot*. PalmSens Knowledgebase. 6th December 2025. URL: https://www.palmsens.com/knowledgebase-article/bode-and-nyquist-plot/.

[41] Georgios Tsotridis and Alberto Pilenga. *EU Harmonised Protocols for Testing of Low Temperature Water Electrolysers*. Tech. rep. EUR 30752 EN. Publications Office of the European Union, 2021. DOI: 10.2760/58880. URL: https://op.europa.eu/en/publication-detail/-/publication/bbbeba00-ee82-11eb-a71c-01aa75ed71a1.

[42] S. Shiva Kumar et al. “Experimental and simulation of PEM water electrolyser with Pd/PN-CNPs electrodes for hydrogen evolution reaction: Performance assessment and validation”. In: *International Journal of Hydrogen Energy* 348 (2024). Available online. DOI: https://doi.org/10.1016/j.apenergy.2023.121565.

[43] M. Maier et al. “Mass transport in PEM water electrolysers: A review”. In: *International Journal of Hydrogen Energy* 47.1 (2022), pp. 30–56. DOI: 10.1016/j.ijhydene.2021.10.013. URL: https://doi.org/10.1016/j.ijhydene.2021.10.013.

[44] Damien Guilbert et al. “Modeling of the Dynamic Behavior of a PEM Electrolyzer”. In: *Proceedings of the 2022 International Conference on Smart Cities (ICSC)*. IEEE, 2022, pp. 1–6. DOI: 10.1109/ICSC57768.2022.9993944. URL: https://doi.org/10.1109/ICSC57768.2022.9993944.

[45] Elliot Padgett et al. “Quantifying Sources of Voltage Decay in Long-Term Durability Testing for PEM Water Electrolysis”. In: *Journal of The Electrochemical Society* 172 (2025), p. 054508. DOI: https://iopscience.iop.org/volume/1945-7111/172.

[46] Michel Suermann, Thomas J. Schmidt, and Felix N. Büchi. “Investigation of Mass Transport Losses in Polymer Electrolyte Electrolysis Cells”. In: *ECS Transactions* 69.17 (2015), pp. 1141–1148. DOI: 10.1149/06917.1141ecst.

[47] James L. Young et al. “PEM electrolyzer characterization with carbon-based hardware and material sets”. In: *Electrochemistry Communications* 124 (2021), p. 106941. DOI: 10.1016/j.elecom.2021.106941.

[48] J. Kleemann, F. Finsterwalder, and W. Tillmetz. “Characterisation of mechanical behaviour and coupled electrical properties of polymer electrolyte membrane fuel cell gas diffusion layers”. In: *Journal of Power Sources* 190.1 (2009), pp. 92–102. DOI: https://doi.org/10.1016/j.jpowsour.2008.09.026.

[49] Malte Pfennig, Barbara Schiffer, and Tanja Clees. “Thermodynamical and electrochemical model of a PEM electrolyzer plant in the megawatt range with a literature analysis of the fitting parameters”. In: *International Journal of Hydrogen Energy* 104 (2025), pp. 567–583. DOI: 10.1016/j.ijhydene.2024.04.335.

[50] S. Slade et al. "Ionic Conductivity of an Extruded Nafion 1100 EW Series of Membranes". In: *Journal of The Electrochemical Society* 149.12 (2002), A1556. DOI: 10.1149/1.1517281.

Appendix

Matlab code for the model

```
clc; clear; close all;

M_H2 = 2.016; %g/mol
z = 2; % e-
F = 96485; %C
Vm = 24.05; %L/mol H2 at 20ºC and 1atm
V_reversible = 1.24;%V
V_thermoneutral = 1.48;%V
R = 8.314;
T_C = 80;
T = T_C + 273.15;
I = 0:1.25:50; %A
current_density = I/25; %A/cm^2

R_shortcut = 0.0778; %Ohm Average resistance, linear increment

%Ohm's Law
V_shortcut = I * R_shortcut; %V

%DATA READING OF NO SHORT CIRCUIT
file2 = 'Nice_IV_curve.csv';
try
    data2 = readmatrix(file2);
    % Columns 4 (Current), 5 (Voltage).
    raw2 = data2(:, [4, 5]);
    clean2 = rmmissing(raw2);
    cd2 = clean2(:, 1) / 25;
    v2 = clean2(:, 2);
catch
    disp(['Error reading ', file2]);
    cd2 = []; v2 = [];
end

for i = 1:length(I)
    if V_shortcut(i) > V_thermoneutral
        H2_prod_ohm(i) = I(i) * 2.016 / (z*F);
    else
         H2_prod_ohm(i) = 0;
```

```
    end
end

%DATA READ SHORT CIRCUIT
filename = '10_11_IV_curve.xlsx';
try
    data = readmatrix(filename);
catch ME
    disp('Error: Could not read the file.')
    disp('Make sure the file "First experimental IV-curve data.xlsx - Sheet1.csv" is in the
    rethrow(ME)
end

h2_production_exp = data(:, 4); %NLPM
h2_production_exp = h2_production_exp(~isnan(h2_production_exp)); %Filter to not have NaN
voltage_exp = data(:, 3); %V
voltage_exp = voltage_exp(~isnan(voltage_exp));%filter
I_exp = data(:, 2); %A
I_exp = I_exp(~isnan(I_exp)); %filter

I_ec = (h2_production_exp ./ 60) ./ Vm .* z .* F; %Current used to produce hydrogen (A)

I_loss = I_exp - I_ec; %Current applied - current used to produced hydrogen = CURRENT LOSSES

I_shorcut = voltage_exp ./ R_shortcut;

h2_production_theo = I_exp .*60 .*Vm ./z ./F;
Fardaic_efficiency = h2_production_exp ./ h2_production_theo;
Faradaic_eff_no_shortcircuit = 0.37 ./h2_production_theo;

%Tafel and exchange current density
eta = voltage_exp - V_reversible;
log_I_ec = log10(I_ec);
log_I_exp = log10(I_exp);
x_tafel = log_I_ec(~isinf(log_I_ec) & ~isnan(log_I_ec)); %Filter when I_ec is 0

y_tafel = eta(eta>0.22); %Filter values for when I_ec > 0

if isempty(x_tafel)
    disp('No hay suficientes datos válidos para calcular i0');
else
    %Lineal regression
    p = polyfit(x_tafel, y_tafel, 1);

    b_slope = p(1);      % Tafel slope
    intercept = p(2);    % Intercept
```

```
    i_0_total = 10^(-intercept / b_slope);

    %Exchange current density calculation
    Area_celda = 25; % cm^2
    j_0 = i_0_total / Area_celda; % [A/cm^2]

   %Plot
 figure('Name', 'Ajuste Tafel Tafel', 'Color', 'w'); hold on;
    plot(x_tafel, y_tafel, 'bo', 'MarkerSize', 8, 'LineWidth', 1.5, ...
        'DisplayName', 'Datos Experimentales (\eta > 0.22V)');
    plot(x_tafel, polyval(p, x_tafel), 'r-', 'LineWidth', 3, ...
        'DisplayName', 'Ajuste Lineal Tafel');


    set(gca, 'FontSize', 16, 'FontWeight', 'bold', 'LineWidth', 1.5);
    grid on; box on;
    xlabel('log_{10}(I_{ec}) [A/cm^2]', 'FontSize', 16, 'FontWeight', 'bold');
    ylabel('Overpotential \eta [V]', 'FontSize', 16, 'FontWeight', 'bold');
    ecuacion_str = { ...
                    ['\eta = ' num2str(b_slope, '%.4f') ' \cdot log(I) + ' num2str(interc
    xlims = xlim; ylims = ylim;
    x_pos = xlims(1) + 0.05 * (xlims(2)-xlims(1));
    y_pos = ylims(1) + 0.90 * (ylims(2)-ylims(1));

    text(x_pos, y_pos, ecuacion_str, ...
        'FontSize', 20, ...
        'FontWeight', 'bold', ...
        'Color', 'k', ...
        'BackgroundColor', 'w', ...
        'EdgeColor', 'k', ...
        'Margin', 5, ...
        'VerticalAlignment', 'top');

    hold off;
end

%%INTERNAL RESISTANCE
valid_idx = ~isnan(I_exp) & ~isnan(voltage_exp);
I_initial = I_exp(I_exp(valid_idx)<19);
V_initial = voltage_exp(voltage_exp(valid_idx)<1.46);
I_after_reaction = I_exp(I_exp(valid_idx)>19);
V_after_reaction = voltage_exp(voltage_exp(valid_idx)>1.46);

p = polyfit(I_initial, V_initial, 1);
R_internal = p(1);
```

```
p2 = polyfit(I_after_reaction, V_after_reaction, 1);

Cell_Area = 25; % cm^2

% 1. Data Filtering and Cleaning
valid_idx = ~isnan(I_exp) & ~isnan(voltage_exp);
I_clean = I_exp(valid_idx);
V_clean = voltage_exp(valid_idx);

% 2. Range Separation before and after reaction based on experiment data
current_threshold = 19; % A
mask_initial = I_clean < current_threshold;
mask_reaction = I_clean >= current_threshold;

% Initial Data
I_initial = I_clean(mask_initial);
V_initial = V_clean(mask_initial);

% Post-Reaction Data
I_after = I_clean(mask_reaction);
V_after = V_clean(mask_reaction);

% Regression
p1 = polyfit(I_initial, V_initial, 1);
R_initial = p1(1);

p2 = polyfit(I_after, V_after, 1);
R_operating = p2(1);
fprintf('Initial Resistance (Pure Short): %.4f Ohms\n', R_initial);
fprintf('Operating Resistance (High Current): %.4f Ohms\n', R_operating);

J_clean = I_clean / Cell_Area;
J_initial = I_initial / Cell_Area;
J_after = I_after / Cell_Area;

figure('Name', 'Faradaic Efficiency Analysis', 'Color', 'w');
hold on;
plot(current_density, Fardaic_efficiency * 100, 'b-o', 'LineWidth', 2, ...
    'MarkerSize', 6, 'MarkerFaceColor', 'b');
set(gca, 'FontSize', 16, 'FontWeight', 'bold');
xlabel('Current Density [A/cm^2]', 'FontSize', 16, 'FontWeight', 'bold');
ylabel('Faradaic Efficiency [%]', 'FontSize', 16, 'FontWeight', 'bold');
grid on;
ylim([0 105]);
xlim([0 max(current_density)*1.1]);
```

```
hold off;

%THEORETICAL IV CURVE
E_rev = V_reversible - 0.0009 * (T_C - 25);

j0_anodo = 1e-4; %1e-6;   % [A/cm2]
j0_catodo = 0.1; %1e-3;  % [A/cm2] &https://www.sciencedirect.com/science/article/pii/S03
alpha = 0.5;

ASR_membrana = 0.15; % [Ohm*cm^2]

j = linspace(0.001, 2, 500); % [A/cm^2]

V_rev = ones(size(j)) * E_rev;

Tafel_slope = (R * T) / (z * alpha * F);
eta_act_anodo = Tafel_slope * log(j ./ j0_anodo);
eta_act_catodo = Tafel_slope * log(j ./ j0_catodo);
V_act = eta_act_anodo + eta_act_catodo;

V_ohm = j .* ASR_membrana;
V_cell_theoretical = V_rev + V_act + V_ohm;
R = 8.314;
T_C = 80;
T = T_C + 273.15;

%No short circuit
p3 = polyfit(cd2, v2, 1);
slope_value3 = p3(1);
x_fit3 = linspace(min(cd2), max(cd2), 100);
y_fit3 = polyval(p3, x_fit3);

figure('Name', 'Dual Resistance Analysis vs Theory', 'Color', 'w');
hold on;

%Plot Theoretical Curve
plot(j, V_cell_theoretical, 'k--', 'LineWidth', 2, ...
    'DisplayName', 'Theoretical Curve');

% Plot Experimental Data
plot(J_clean, V_clean, 'bo', 'MarkerFaceColor', 'b', 'MarkerSize', 6, ...
    'DisplayName', 'Exp. data with short circuit');

plot(cd2, v2, 'ko', ...
    'MarkerFaceColor', 'k', ...
    'MarkerSize', 6, ...
```

```
    'DisplayName', 'Exp. data no short circuit');

plot(x_fit3, y_fit3, 'y-', ...
    'LineWidth', 2.5, ...
    'DisplayName', sprintf('Resistance no short circuit: %.4f \\Omega*cm^2', slope_value3));
xlim([0 2]);

%Plot Fit 1
x_fit1_J = linspace(min(J_initial), max(J_initial), 50);
y_fit1 = polyval(p1, x_fit1_J * Cell_Area);
plot(x_fit1_J, y_fit1, 'r-', 'LineWidth', 2.5, ...
    'DisplayName', sprintf('Initial Resistance: %.4f \\Omega*cm^2', R_initial));

%Plot Fit 2
x_fit2_J = linspace(min(J_after), max(J_after), 50);
y_fit2 = polyval(p2, x_fit2_J * Cell_Area);
plot(x_fit2_J, y_fit2, 'g-', 'LineWidth', 2.5, ...
    'DisplayName', sprintf('Operating Resistance: %.4f \\Omega*cm^2', R_operating));

set(gca, 'FontSize', 16, 'FontWeight', 'bold');
xlabel('Current Density [A/cm^2]', 'FontSize', 16, 'FontWeight', 'bold');
ylabel('Voltage [V]', 'FontSize', 16, 'FontWeight', 'bold');
legend('Location', 'southeast', 'FontSize', 16);
grid on;
box on;
ylim([0 3.0]);
hold off;
```